



**CALL FOR  
PAPERS**



**It aims to publish original, theoretical and practical advances in :**

**Computer Science & Engineering  
Information Technology  
Information System  
Electrical and Electronics Engineering  
Electronics and Telecommunication  
Mechanical Engineering  
Civil Engineering  
Industrial Engineering  
all interdisciplinary streams of Engineering Sciences.**

**Yayasan Riset dan Pengembangan Intelektual (YRPI)  
2019**

## Journal of Applied Engineering and Technological Science (JAETS)

[Current](#) [Archives](#) [About the Journal](#) [Editorial Team](#) [Announcements](#) [Privacy Statement](#) [Submissions](#) [Contact](#)

[Q Search](#)

[Home](#) / [About the Journal](#)

### About the Journal

Journal of Applied Engineering and Technological Science (JAETS) is published by Yayasan Pendidikan Riset dan Pengembangan Intelektual (YRPI), Pekanbaru, Indonesia. It is academic, online, open access, peer reviewed international journal. It aims to publish original, theoretical and practical advances in Computer Science & Engineering, Information Technology, Electrical and Electronics Engineering, Electronics and Telecommunication, Mechanical Engineering, Civil Engineering, Textile Engineering and all interdisciplinary streams of Engineering Sciences. Journal of Applied Engineering and Technological Science (JAETS) is published annually 2 times every June and Desember.

<https://www.scopus.com/sourceid/21101138527>



#### Journal Info :

Journal Title	: Journal of Applied Engineering and Technological Science : (JAETS)
Initials	: JAETS
Frequency	: 2 issues per year (December and June)
DOI	: by  Crossref with Prefix 10.37385( <a href="https://doi.org/10.37385/jaets">https://doi.org/10.37385/jaets</a> )
Print ISSN	: 2715-6087
Online ISSN	: 2715-6079
Editor-in-chief	: <a href="#">Dr. Muhammad Luthfi Hamzah, B.T., M.Kom</a>
Publisher	: Yayasan Riset dan Pengembangan Intelektual (YRPI)
Language	: English
Fee of Charge	: USD 450
Indexing	: <a href="#">Scopus</a>   <a href="#">DOI</a>   <a href="#">Google Scholar</a>   <a href="#">Garuda</a>   <a href="#">Moraref</a>   <a href="#">IndexCopernicus</a>   <a href="#">WorldCat</a>   <a href="#">DRJ</a>
Citation Analysis	: <a href="#">SCIT</a>   <a href="#">Dimensions</a>
	: <a href="#">Scopus</a>   <a href="#">Web of Science</a>   <a href="#">Google Scholar</a>   <a href="#">Dimensions</a>

Journal of Applied  
Engineering and...

**Q4** Computer Science  
(miscellaneous)

SJR 2023  
0.14  
powered by scimagojr.com

1.4 2022  
CiteScore

27th percentile  
Powered by Scopus



#### ADDITIONAL MENU

[FOCUS AND SCOPE](#)

[EDITORIAL TEAM](#)

[PUBLICATION ETHIC](#)

Editorial Team: <https://journal.yrpioku.com/index.php/jaets/about/editorialTeam>

## Journal of Applied Engineering and Technological Science (JAETS)

[Current](#) [Archives](#) [About the Journal](#) [Editorial Team](#) [Announcements](#) [Privacy Statement](#) [Submissions](#)

[Home](#) / [Editorial Team](#)

### Editorial Team

#### Editor in Chief :

Dr. Muhammad Luthfi Hamzah, B.IT, M.Kom Universitas Islam Negeri Sultan Syarif Kasim, Indonesia. [Scopus ID : 57211346531](#)

#### Editor Board :

Prof. Dr. V.D. Ambeth Kumar, Panimalar Engineering College, India. [Scopus ID : 37100924000](#)

Carlos Hernán Fajardo-Toro, PhD. Universidade de Vigo, Spain. [Scopus ID : 57215501173](#)

Ghazala Ishrat, Ph.D (Habib University), Pakistan. [Scopus ID : 57211030470](#)

R. Seenivasan, Ph.D (Madurai Kamaraj University), India. [Scopus ID : 57209451482](#)

Dr. Ghazala Ishrat, Jamia Millia Islamia, India. [Google Scholar](#)

Jhoselle Tus, St. Paul College of Bocaue, Philippines. [Google Scholar](#)

[Shatha Hussain](#), City University College of Ajman, Uni Emirat Arab

Dr. Rado Yendra, Universitas Islam Negeri Sultan Syarif Kasim, Indonesia. [Scopus ID : 55670887600](#)

Muhammad Israr Fathoni, Universiti Kebangsaan Malaysia, Malaysia. [Scopus ID : 57194045723](#)

Dr. Al Hamidy Hazidar, MIT, Universiti Kebangsaan Malaysia, Malaysia. [Scopus ID : 57213521384](#)

Mohammed Saud Mira, Independent researcher, Saudi Arabia. [Scopus ID : 57205345714](#)

Sutoyo, Universitas Islam Negeri Sultan Syarif Kasim Riau, Indonesia. [Scopus ID 57142558400](#)

Afriansyah, Universitas Lancang Kuning, Indonesia. [google scholar](#)

Syaiful Islami, Universitas Negeri Padang, Indonesia. [Scopus : 57207300018](#)

Anofrizen, Universitas Islam Negeri Sultan Syarif Kasim Riau, Indonesia. [Scopus : 57194573991](#)

Muh Anhar, Politeknik Negeri Ketapang, Indonesia. [Google Scholar](#)

Assoc. Prof. Dr. Hamzah, Universitas Islam Riau, Indonesia. [Scopus ID 57205297973](#)

Dr. Hastuti Marlina, Sekolah Tinggi Ilmu Kesehatan Hang Tuah Pekanbaru, Indonesia. [Scopus ID 57194596691](#)

Nesdi Evrilyan Rozanda, Universitas Islam Negeri Sultan Syarif Kasim Riau, Indonesia. [Scopus ID : 56464326000](#)

Irohito Nozomi, Universitas Putra Indonesia YPTK Padang, Indonesia. [Scopus ID : 57222902170](#)

Cendra Wadisman, Universitas Putra Indonesia YPTK Padang, Indonesia. [Scopus ID : 57222898934](#)

Dr. Zulfadli Hamzah, Universitas Islam Riau, Indonesia. [Scopus ID 57044487600](#)

Dr. Wenny Marthiana, ST, MT. Universitas Bung Hatta, Indonesia. [Scopus ID : 57201862378](#)

#### Associate Editors :

Dr. B.V. Santhosh Krishna, Department of ECE, New Horizon College of Engineering, Bengaluru, Karnataka, India, [Scopus ID : 56888824700](#)

Abdessalam EL YASSINI, Ph.D, Faculté des Sciences Semlalia, Cadi Ayyad University, Morocco, [Scopus ID : 57194680626](#)

Asst. Prof. Khongdet Phasinam, Ph.D., Pibulsongkram Rajabhat University, Thailand, [Scopus ID : 57225180258](#)

Dr. Batara, Tong Ji University, Shanghai, China, [Scopus ID : 57202757895](#)

Dr. Leo John F, Prowess University, United States, [Scopus ID : 7004377227](#)

Mr. Ronak Gandhi, ITM Vocational University, Vadodara, India, [Scopus ID : 57208575257](#)



**Ibrahim Hanaish, Misuratu University, Libya [Scopus ID : 54405615400](#)**

**Assoc. Prof. Dr. Wan Zawiah Wan Zin , Universiti Kebangsaan Malaysia, Malaysia [Scopus ID : 24465955700](#)**

**Anton Abdulbasah Kamil, Istanbul Gelisim University, Turkey [Scopus ID : 24481107300](#)**

**Gusman Nawanir, P.hD, Universiti Malaysia Pahang, Malaysia [Scopus ID : 55887973700](#)**

**Abhay Pratap Singh, Gurukula Kangri Vishwavidyalaya, Haridwar, India [Scopus ID : 57215528239](#)**

**Dr. Sunariya Utama, B.IT, M.IT, Universiti Utara Malaysia, Malaysia [Scopus ID : 57190944772](#)**

**Dr. Mahesi Agni Zaus, Universiti Tun Husein Onn Malaysia, Malaysia [Scopus ID 57207312835](#)**

**Dr. Rizky Ema Wulansari, M.Pd.T, Universiti Tun Husein Onn Malaysia, Malaysia [Scopus ID 57193502350](#)**

**Al-Khowarizmi, Universitas Muhammadiyah Sumatera Utara, Indonesia [Scopus ID 57204804487](#)**

**Dr. Zainol Mustafa, Universiti Kebangsaan Malaysia, Malaysia. [Scopus ID : 36504772800](#)**

**Prof. Dr. Okfalisa, Universitas Islam Negeri Sultan Syarif Kasim Riau, Indonesia. [Scopus ID : 35102923400](#)**

**Dr. Astri Ayu Purwati, M.Sc, Institut Bisnis dan Teknologi Pelita Indonesia, Indonesia [Scopus ID : 57205297859](#)**

**Prof. Dr. Kasman Rukun Universitas Negeri Padang, Indonesia [Scopus ID : 57210974981](#)**

**Dr. Evizal Abdul Kadir. Universitas Islam Riau, Indonesia [Scopus ID : 50561254400](#)**

**Dr. Abdullah Bin Husin. Universitas Islam Indragiri, Indonesia [Scopus ID : 57206889771](#)**

**Prof. Dr. Ambiyar, Universitas Negeri Padang, Indonesia [Scopus ID : 57207299138](#)**

**Dr. Arif Ridho Lubis, Politeknik Negeri Medan, Indonesia [Scopus ID : 57188875498](#)**

**Dr. Yahfizham, ST, M.Cs, Universitas Islam Negeri Sumatera Utara, Indonesia [Scopus ID : 57201748107](#)**

**Dr. Edi Septe, MT, Universitas Bung Hatta, Indonesia [Scopus ID : 56119695800](#)**

**Dr. Suryadimal, MT, Universitas Bung Hatta, Indonesia [Scopus ID : 57205216028](#)**

**Muhammad Marizal, Universitas Islam Negeri Sultan Syarif Kasim, Riau, Indonesia [Scopus ID 57192941205](#)**

**Dr. Rukin, Universitas Teknologi Surabaya, Indonesia [Sinta](#)**

**Dr. Yenny Desnelita, M.Kom, Institut Bisnis dan Teknologi Pelita Indonesia, Indonesia** [Scopus ID : 57200088180](#)

**Dr. Yogi Yunefri, M.Kom, Universitas Lancang Kuning, Indonesia** [Scopus ID : 57200089157](#)

**Assoc. Prof. Dr. Astri Ayu Purwati, M.Sc, Institut Bisnis dan Teknologi Pelita Indonesia, Indonesia** [Scopus ID : 57205297859](#)

**Assoc. Prof. Dr. Alex Wenda, ST., M.Eng, Universitas Islam Negeri Sultan Syarif Kasim Riau, Indonesia.** [Scopus ID : 57207458490](#)



## Vol. 6 No. 1 (2024): Journal of Applied Engineering and Technological Science (JAETS)

The author's countries are coming from **Kuwait** (American University of the Middle East), **United Kingdom** (Nottingham Trent University), **Taiwan** (National Chung Hsing University), **Australia** (Western Sydney University), **Vietnam** (Hanoi University of Industry, Phenikaa University, Vietnam Academy of Science and Technology, Vietnam National Post and Telecommunication Group), **Malaysia** (Sultan Idris Education University, Universiti Kebangsaan Malaysia, Higher Institution Centre of Excellence (HICoE), UM Power Energy Dedicated Advanced Centre (UMPEDAC), Universiti Tun Hussein Onn Malaysia), **Iraq** (Al-Nahrain University, University of Baghdad, Al-Mansour University College Baghdad), **Morocco** (University Mohammed V in Rabat (UM5), University Chouaib Doukkali of El Jadida), **Peru** (UNIVERSIDAD NACIONAL DEL CALLAO, UNIVERSIDAD CIENCIAS Y HUMANIDADES, UNIVERSIDAD CESAR VALLEJO), **India** (Lyalpur Khalsa College Technical Campus, Mepco Schlenk Engineering College, Panimalar Engineering College, SRM Institute of Science and Technology, KCG College of Technology, Adithya Institute of Technology, Dayananda Sagar University, Hindustan College of Arts and Science, Thiagarajar College of Engineering, Jyothi Engineering College, Sri Venkateswara College of Engineering & Technology (A), Loyola Institute of Technology and Science R. M. K. College of Engineering and Technology, Noorul Islam Centre for Higher Education, R. M. K. College of Engineering and Technology, S.T.Hindu College, Erode Sengunthar Engineering College S.A. Engineering College, Symbiosis Institute of Business Management, Amity University), **Myanmar** (Yangon Technological University), **Thailand** (Ramkhamhaeng University, Rajamangala University of Technology Lanna Tak, Chiang Mai University, Sripatum University), **Brunei Darussalam** (Universiti Islam Sultan Sharif Ali), **Bangladesh** (Jahangirnagar University), **Indonesia** (Universitas Gadjah Mada, Research Center for Nuclear Reactor Technology, National Research and Innovation Agency, Indonesia, Universitas Padjadjaran, Politeknik Manufaktur Bandung, Institut Teknologi Sepuluh Nopember, Bina Nusantara University, Universitas Hasanuddin, Universitas Andalas, Universitas Negeri Padang, Universitas Islam Negeri Sultan Syarif Kasim Riau, Institut Teknologi Telkom Purwokerto, Institut Agama Islam Negeri Curup, Institut Agama Islam Negeri Kerinci, Universitas Riau, Universitas Tadulako, Universitas Samudra, Universitas Lancang Kuning, Universitas Mulawarman, Universitas Sains dan Teknologi Indonesia, Universitas Hang Tuah Pekanbaru, Marine and Fisheries Polytechnic Sorong, Sorong Muhammadiyah University of Education, Marine and Fisheries Polytechnic Kupang, Marine and Fisheries Polytechnic Bone, Sebelas Maret University, Airlangga University, Telkom University, Purwokerto, Universitas Semarang, Politeknik Negeri Malang, University of Pembangunan Nasional (UPN) Veteran Yogyakarta, University of Bengkulu, Universitas Medan Area, Universitas Sumatera Utara, HKBP Nommensen University, Politeknik ATI Padang)

DOI: <https://doi.org/10.37385/jaets.v6i1>

Published: 2024-12-15

### Articles

#### On The Assembly Line Balancing Problem: A Simplified Perspective With The Precedence Matrix

Magdy Helal, Kaushik Nag, Rifat Ozdemir

1-20





### Mobile Tourism Research and Practices: A Comprehensive Bibliometric Exploration and Future Study Direction

Syaifullah Syaifullah, Shamsul Arrieya Ariffin, Norhisham Mohamad Nordin

21-47

 PDF

### Development of an Optimized Ensemble Least Squares Model for Identifying Potential Deposit Customers

Firman Aziz, Mutia Maulida, Jafar Jafar, Nurafni Shahnyb, Norma Nasir, Ampauleng Ampauleng

48-59

 PDF

### Pre-trained BERT Architecture Analysis for Indonesian Question Answer Model

Sudianto Sudianto

60-68

 PDF

### An Enhanced Image Segmentation Technique-Based on Motion Detection Algorithm

Zaid Sh. Bakr, Hamzah M. Marhoon, Ammar Alaythawy

69-85

 PDF

### Air-Gap Reduction and Antenna Positioning of an X-Band Bow Tie Slot Antenna on 2U CubeSats

Boutaina Benhmimou, Fouad Omari, Nancy Gupta, Khalid El Khadiri, Rachid Ahl Laamara, Mohamed El Bakkali

86-102

 PDF

### Scene Text Detection and Recognition Using Maximally Stable Extremal Region

Golda Jeyasheeli P, Athinarayanan B, Manish T, Mohamad Umar M

103-114

 PDF

### Multimodal Analysis of Augmented Reality in Basic Programming Course: Innovation Learning in Modern Classes

Rizky Ema Wulansari, Rizki Hardian Sakti, Hasep Saputra, Agariadne Dwinggo Samala, Rifyal Novalia, Hla Myo Tun

115-137

 PDF

---

**Software Design for Inventory Management Improvement in a Peruvian National University**

Linett Velasquez, Santiago Rubiños, Junior Grados, Juan Grados, Claudia Marujo

138-154

 PDF

**Environmental Quality Impact Analysis of Settlements Bontang Kuala, East Kalimantan Province**

Andrew Stefano, Triyatni Martosenjoyo, Idawarni Asmal, Edward Syarif

155-173

 PDF

**Does Social Presence on Social Commerce Platform Attract Buying Intention of Indonesian Local Food?**

Ratni Prima Lita, Meuthia Meuthia, Devi Yulia Rahmi, M. Fajar Syafrida

174-191

 PDF

**Interactive Geographic Visualization and Unsupervised Learning for Optimal Assignment of Preachers to Appropriate Congregations**

Rahmad Kurniawan, Ibnu Daqiqil ID, Abdul Somad Batubara, Fitra Lestari, Arisman Adnan, Fatayat Fatayat, Ilyas Husti

192-205

 PDF

**Investigating Tensile Strength in SLA 3D Printing Enhancement Through Experimentation and Finite Element Analysis**

Siwasit Pitjamit, Norrapon Vichiansan, Parida Jewpanya, Pinit Nuangpirom, Pakpoom Jaichomphu, Komgrit Leksakul, Pattarawadee Poolperm

206-224

 PDF

**Sara Detection on Social Media Using Deep Learning Algorithm Development**

M. Khairul Anam, Lucky Lhaura Van FC, Hamdani Hamdani, Rahmadden Rahmadden, Junadhi Junadhi, Muhammad Bambang Firdaus, Irwanda Syahputra, Yuda Irawan

225-237

 PDF

### **Effect of Zinc Addition in Copper to Structure, Hardness, Corrosion, and Antibacterial Activity**

Lisa Samura, Mustamina Maulani, Cahaya Rosyidan, Kartika Fajarwati Hartono, Suryo Prakoso, Evi Ulina Margareta Situmorang, Daniel Edbert, Bambang Soegijono, Muhammad Yunan Hasbi, Ferry Budhi Susetyo 465-479

 PDF

### **Proximity Index Value for Supplier Selection Using Compromise Weighting of Stepwise Weight Assessment Ratio Analysis and The Method of Removal Effects Of Criteria: A Case Study in Indonesian Leather Industry**

Agus Ristono 480-498

 PDF

### **Development of A Low-Cost Analyzer for Misalignment Identification Based on Vibration and Current Analysis**

Dedi Suryadi, Acraz M Bahrums, Novalio Daratha, Radzi Ambar 499-507

 PDF

### **Development of Potato Nano Carbon as Electrode for Supercapacitors Achieves Green-Sustainable Development Goals**

Indri Dayana, Dadan Ramdan, Moranain Mungkin, Habib Satria, Muhammad Fadlan Siregar, Martha Rianna, Juliaster Marbun, Siti Utari Rahayu 508-518

 PDF

### **Supply Chain Conceptual Model to Optimize a Local Food Agroindustry from the Coconut Milk Processing**

Meilizar Meilizar, Rika Ampuh Hadiguna, Santosa Santosa, Nofialdi Nofialdi 519-536

 PDF

### **Innovative Tech-Savvy Education: Designing a Smart Assessment System**

Syaiful Islami, Ambiyar Ambiyar, Sukardi Sukardi, Anggi Agni Zaus, Anggun Agni Zaus, Mahesi Agni Zaus 537-549

 PDF



## ***EFFECT OF ZINC ADDITION IN COPPER TO STRUCTURE, HARDNESS, CORROSION, AND ANTIBACTERIAL ACTIVITY***

**Lisa Samura<sup>1\*</sup>, Mustamina Maulani<sup>2</sup>, Cahaya Rosyidan<sup>3</sup>, Kartika Fajarwati Hartono<sup>4</sup>, Suryo Prakoso<sup>5</sup>, Evi Ulina Margareta Situmorang<sup>6</sup>, Daniel Edbert<sup>7</sup>, Bambang Soegijono<sup>8</sup>, Muhammad Yunan Hasbi<sup>9</sup>, Ferry Budhi Susetyo<sup>10</sup>**

Department of Petroleum Engineering, Universitas Trisakti, 11440, Indonesia<sup>12345</sup>

Department of Physiology School of Medicine and Health Sciences, Atma Jaya Catholic University of Indonesia, 14440, Indonesia<sup>6</sup>

Department of Microbiology, Atma Jaya Catholic University of Indonesia, 14440, Indonesia<sup>7</sup>

PROUDTEK Lab., Department of Geoscience, Universitas Indonesia, 16424, Indonesia<sup>8</sup>

Research Center for Metallurgy – National Research and Innovation Agency, 15314, Indonesia<sup>9</sup>

Department of Mechanical Engineering, Universitas Negeri Jakarta, 13220, Indonesia<sup>10</sup>

[lisa.samura@trisakti.ac.id](mailto:lisa.samura@trisakti.ac.id)<sup>1</sup>

Received: 12 September 2024, Revised: 17 November 2024, Accepted: 19 November 2024

*\*Corresponding Author*

---

### **ABSTRACT**

*Brass (CuZn) is widely used today due to better mechanical, thermal, and chemical properties. The present research fabricated CuZn alloy by adding various Zn (6, 9, and 12 wt.%) to the Cu using gravity casting. Casts CuZn alloy by adding various Zn to the Cu to investigate optimum composition were resulting highest inhibited of bacterial activity. In addition, the structure, hardness, and electrochemical behavior of the alloy were also investigated using XRD, Vickers hardness, and potentiostat equipment. XRD confirmed that CuZn alloy has an alpha phase, and a FCC crystal structure. The rise of the Zn content in the alloy led to an increase in crystallite size, a decrease in the hardness and a shift to a more negative OCP potential at 1200 s measurement. Enhancing the Zn content to 9 wt.% in the alloy lead to decrease the corrosion rate. Moreover, 24-hour post-contact observation found that the sample places removed remained clear of bacteria. The Cu6Zn sample successfully inhibited the growth of Escherichia coli in the 3<sup>rd</sup> hour, while Staphylococcus aureus was 100 % reduced in the 7<sup>th</sup> hour. The Cu6Zn sample could be used as an alternative material for medical equipment in ambulances.*

**Keywords:** *XRD, Vickers, Electrochemical Measurement, Staphylococcus Aureus, Escherichia Coli*

### **1. Introduction**

Brass (CuZn) is an alloy widely used in the national defense, oil and gas industries, and health because it has better mechanical properties, thermal conductivity, and corrosion resistance (Bhavsar & Bali, 2023; Wang et al., 2023; Widyastuti et al., 2023). CuZn alloys for medical equipment in transportation such as ambulances need to consider two parameters: corrosion resistance and antibacterial characteristics. Commonly NaCl media was used to investigate corrosion for ambulance equipment. This condition due to ambulance equipment commonly exposure from medical patients



eccrine sweat and saline-infused (Baker & Wolfe, 2020; Tayyab et al., 2021). Furthermore, some studies found that after cleaning the ambulance, 35.37 % of bacterial contaminants were still seen (Syamsuir et al., 2023).

Viegas et al. found *Staphylococcus aureus* was detectable on firefighter's ambulance equipment (Viegas et al., 2021). *Staphylococcus aureus* is a type of bacteria that could cause skin disease and is hard to treat with traditional antibiotics. *Staphylococcus aureus* bacteria tend to have methicillin resistance. According to Tajik et al., 38.4 % of *Staphylococcus aureus* methicillin resistant was found in Tehran community (Tajik et al., 2020). Moreover, this bacteria also could contaminate orthopedic implants and cause serious infections (Pietrocola et al., 2022).

Several researchers were interested in investigating the corrosion behavior of CuZn alloy in NaCl medium (Abed & Dawood, 2022; Chen et al., 2024; Gao et al., 2021; Yin et al., 2021). Abed and Dawood investigated the corrosion behavior of Cu40Zn alloy in 3.5% NaCl and found a corrosion rate of around 0.037 mmpy (Abed & Dawood, 2022). Yin et al. investigated the corrosion behavior of Cu alloy in NaCl medium were immersed in different times. More time is immersed, resulting in more corrosion resistance of Cu (Yin et al., 2021). Chen et al. investigated Cu alloy in NaCl medium and found Cu potential around -0.305 V vs SCE and Zn potential around -1.165 V vs SCE (Chen et al., 2024). Gao et al. found that a reduction in thickness (50 to 60 %) of CuZn using cold rolling resulted in a significant decrease in corrosion current from 4.824 to 1.804  $\mu\text{A}/\text{cm}^2$  (investigating in 3.5 % NaCl) (Gao et al., 2021). Moreover, aluminum (Al) alloy widely used in transportation sector such as ambulance (Blanco et al., 2022; Vandersluis et al., 2020). Liu et al. have found Al alloy corrosion current between 4.8685.251 A/cm<sup>2</sup> in a 3.5% NaCl medium (Liu et al., 2020). Comparing the studies of Liu et al. and Gao et al., Al alloy has a higher corrosion current than CuZn (Gao et al., 2021; Liu et al., 2020). Corrosion current significantly influences the corrosion rate, and a rise in the corrosion current would enhance the corrosion rate.

Recently, researchers have been interested in investigating CuZn alloy for medical applications (Azizian et al., 2024; Riaz et al., 2024; Sabbouh et al., 2023). Azizian et al. investigated CuZn alloys microstructure, mechanical properties and cytotoxicity for cardiovascular applications (Azizian et al., 2024). Riaz et al. investigated the structural and biological properties of CuZn alloy for orthopedic applications (Riaz et al., 2024). Moreover, Sabbouh et al. did the sonification of CuZn in an alkali solution to enhance the antibacterial inhibition zone (Sabbouh et al., 2023). Moreover, Syamsuir et al. have investigated the antibacterial activity of *Staphylococcus aureus* by presenting a Cu layer for ambulance equipment (Syamsuir et al., 2023).

The killing mechanism of bacterial activity inseparable from the ions released by the alloy (Qu et al., 2020). Cu<sup>2+</sup> ions could be adsorbed on the cytoplasmic membrane surfaces, then penetrate the bacteria, react with sulfhydryl groups, and cause the cell to die (Zeng et al., 2022). The released Zn<sup>2+</sup> ions could penetrate the cell membrane and cause cell death (Du et al., 2021). Zhang et al. have stated that Cu<sup>2+</sup> and Zn<sup>2+</sup> ions could act as antibacterial agents and inhibit *Staphylococcus aureus* growth (Zhang et al., 2021).

According to the literature review, research on CuZn alloys with Zn compositions in the range of 6–12 wt.% for medical transportation purposes has not been thoroughly investigated. As mentioned above, the killing mechanism of bacterial activity depends on Cu and Zn ions. CuZn alloy can transform into Cu and Zn ions. Therefore, the present research casts CuZn alloy by adding various Zn to the Cu to investigate optimum composition, resulting in a higher killing mechanism of bacterial activity. Moreover, different alloy compositions would result in different electrochemical behavior and mechanical properties. The present study investigated structure, hardness, electrochemical behavior, and antibacterial activity using X-ray diffraction (XRD), Vickers hardness equipment, potentiostat, and digital camera.

## **2. Literature Review**

Many techniques are used to make CuZn alloys, including gravity and investment casting (Hendrawan et al., 2021; Ziat et al., 2020). Gravity casting is simple, inexpensive, and can rapidly fill complex geometry (Huang et al., 2024; Nuryadi et al., 2020). Moreover, in the fabrication of CuZn alloys, one thing needs to be considered to produce specific properties, namely alloy composition. Researchers focused on adding various Zn compositions onto Cu for different purposes. Strzpek et al. investigated the mechanical properties of Cu and alpha brass (Cu<sub>2.5</sub>Zn and Cu<sub>6.5</sub>Zn) wire ( $\phi$  3.8 mm). Increased Zn content causes increases in ultimate tensile strength, yield strength and hardness (Strzpek et al., 2019). Situmorang et al. fabricated Cu with various Zn additions (10, 20, 38, and 45 wt.%) and found that the higher the Zn composition, the higher the antibacterial properties (Situmorang et al., 2019). Iqbal et al. melted Cu<sub>28.7</sub>Zn using a furnace and cast to investigate hardness and morphology (Iqbal et al., 2021). Shahriyari et al. added Zn (5, 15, 20, and 30 wt.%), increasing the hardness due to the alloy's rise in the Zn content (Shahriyari et al., 2022). Akhyar et al. melted Cu<sub>28.7</sub>Zn using a gas furnace and cast to investigate the tensile strength (Akhyar et al., 2023). Morath et al. have created Zn<sub>0.8</sub>Cu and Zn<sub>1.5</sub>Cu using casting methods to investigate the biological aspect of arterial implants (Morath et al., 2024). Azizian et al. have added Cu with compositions 1, 2, and

5 wt.% to CuZn alloy by melting in the induction furnace to investigate microstructure, mechanical properties, and cytotoxicity for cardiovascular application (Azizian et al., 2024). Generally, a CuZn alloy with a Zn composition of less than 37 wt.% would produce a single alpha phase with an FCC crystal structure (Clement & Auger, 2023; Mousavi et al., 2020).

## **3. Research Methods**

### **3.1 Material Preparation**

Cu ingot (98.798 %) and Zn powder (99 %) were melted and cast with the alloy composition Cu<sub>x</sub>Zn (x=0, 6, 9, and 12 wt.%, namely as Cu, Cu<sub>6</sub>Zn, Cu<sub>9</sub>Zn, and Cu<sub>12</sub>Zn, respectively) and then confirmed the formed alloy using XRF (Table 1). Before melting was conducted, the ingot and the apparatus, such as the crucible, were cleaned using water to avoid impurities and then dried. The Cu ingot was first filled into a silicon carbide crucible (3kg) and then inserted into a muffle furnace. Melting was carried out in a crucible at 1100 °C under atmospheric pressure. After the Cu has melted, remove it from the muffle furnace, mix it with Zn powder, stir it manually, and pour it into a permanent mold. For comparison, Cu

ingot was melted and poured into a permanent mold without Zn addition. The as-cast ingots were cut for further characterization, such as XRD, hardness, electrochemical measurement, and antibacterial activity observation.

Table 1 –  
various

Sample	Cu	Zn	Al	Si	P	Fe
Cu	98.798	-	0.135	0.444	0.384	0.238
Cu6Zn	92.308	6.384	0.135	0.444	0.384	0.345
Cu9Zn	89.228	9.497	0.135	0.444	0.384	0.312
Cu12Zn	87.075	11.557	0.135	0.444	0.384	0.405

Chemical composition of  
casting samples.  
Element (wt.%)

### 3.2 XRD Measurement

XRD was measured using the PANalytical (Cu K $\alpha$ 1  $\lambda$ =1.5405980) apparatus. XRD was scanned from 20 to 100 $^\circ$ , using step size 0.0217 $^\circ$ . The Highscore software was used to refine and collect peak, phase and crystallographic parameters of as-cast samples. By using that software, full width at half maximum (FWHM) are also found. FWHM data is used to calculate crystallite size.

### 3.3 Hardness Measurement

Before testing, samples with 20 $\times$ 20 $\times$ 6 mm dimensions were polished using silicon carbide up to #3000 grit. Afterward, the polished sample was cleaned using water, followed by alcohol, and then dried using drier equipment. The hardness test was conducted using the Vickers method. An FV-300e hardness test was performed on top of various samples using 1 kg of load. Ten repeatable measurements were conducted.

### 3.4 Electrochemical Measurement

Two electrochemical measurements were conducted in the present research, such as open circuit potential (OCP) and Linear sweep voltammetry (LSV), using Digi-Ivy (DY2311) potentiostat in 0.9 % NaCl at room temperature. OCP was scanned until 1200 s using a sampling scan rate of 0.02 s, while LSV was conducted using a scan rate of 1 mV/s. Cu/CuZn samples are used as the working electrode, platinum wire as the counter electrode, and Ag/AgCl as the reference electrode. LSV data was examined using the Tafel extrapolation method to see corrosion potential ( $E_{corr}$ ) and current density ( $i_{corr}$ ). The corrosion rate could be found by inserting  $i_{corr}$  in the following equation (Soegijono et al., 2020).

$$\text{Corrosion rate (mmpy)} = C \frac{M \times i_{corr}}{\rho \times n} \quad (1)$$

Where C is corrosion constant (3.27 mmpy), M is atomic weight (g/mol),  $\rho$  is material density (g/cm<sup>3</sup>), and n is the number of electrons involved.

### 3.5 Antibacterial Activity Observation

The sample dimension used for antibacterial activity is 20×20×6 mm. Before testing, samples were polished using silicon carbide up to #3000 grit. The experimental procedure for antibacterial activity is similar to that of the previous report (Syamsuir et al., 2023). Moreover, the recent study uses *Staphylococcus aureus* ATCC 25923 for Direct contact kill assay (24 hours) and Fluid contact assay (8 hours). In comparison, *Escherichia coli* 25922 was also used in the present study. Afterward, documentation was captured using a digital camera. In addition, 24-hour post-contact observation and Fluid contact test were also captured using a digital camera.

## 4. Results and Discussions

### 4.1 XRD

The diffraction pattern of Cu/CuZn with (111), (200), (311), and (222) planes can be seen in Figure 1. The four diffraction patterns match the alpha phase, which is shown to align with another study (Heidarzadeh et al., 2022). The acquired XRD data was then analyzed using Highscore software, and the parameters are listed in Table 2. All samples had a face-centered cubic (FCC) crystal structure, indicating that the Cu and Zn atoms dissolve into one another. According to Jinlong et al., the FCC quantity of surface energy is (111)>(001) >(110), and the FCC sample with the (111) plane has the lowest corrosion rate (Jinlong et al., 2016). Moreover, the FCC sample with the preferred orientation of the (111) plane has the highest surface atomic density (Soegijono et al., 2020).

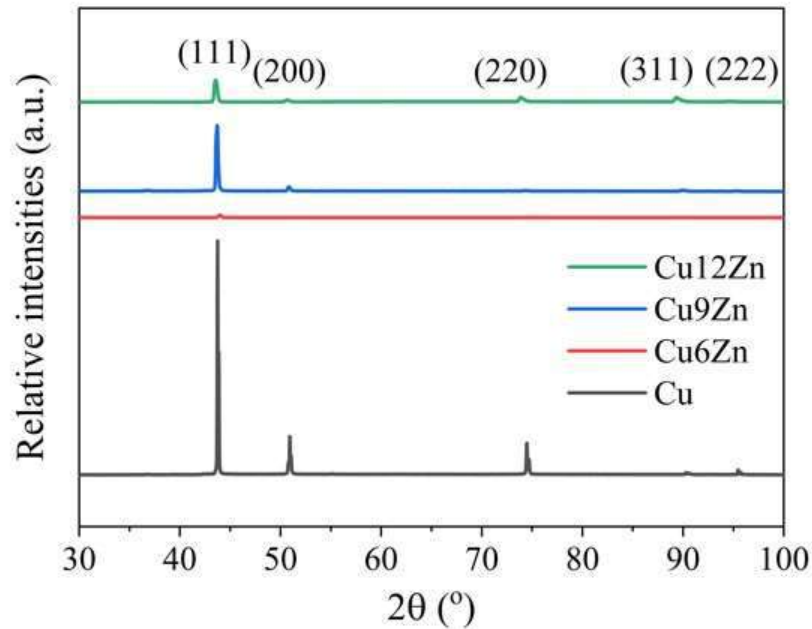


Fig. 1. XRD of various casting samples.

Table 2 - Crystallographic parameters of various casting samples.

Parameter	Sample			
	Cu	Cu6Zn	Cu9Zn	Cu12Zn



Crystal structure	FCC			
Lattice constant $a = b = c$ (Å)	2.964	8.929	2.981	2.964
Cell volume (Å <sup>3</sup> )	26.03	90	26.49	26.05
d-spacing (Å)	1.69	1.18	1.69	2.07
Crystallite Size (nm)	227.20	109.95	204.95	316.26
Micro strain	0.37	0.53	0.16	0.32

Presenting Zn in the alloy reduces crystallite size from 227.20 to 109.95 nm and increases Zn content from 6 to 12 wt.%, leading to an increase in crystallite size from 109.95 to 316.26 nm. This behavior is similar to Özdemiş and Karahan's study that showed Zn in the alloy leads to decreased crystallite size, and an increase in Zn content in the alloy leads to increased crystallite size (Özdemiş & Karahan, 2014). Moreover, the microstrains of the as-cast sample are independent of Zn content, which perfectly agrees with Karahan and Özdemiş's study ((Karahan & Özdemiş, 2014). The smallest microstrain is seen in the Cu<sub>9</sub>Zn sample.

#### 4.2 Hardness

Figure 2 shows the average hardness of various casting samples. Nikhil et al. have found that pure Cu has a hardness of 140 HV when treated at 400 and 600 °C and then held for two hours, followed by quenching in tap water, resulting in a hardness of 100 and 60 HV (Nikhil et al., 2021). The higher heat treatment temperatures led to a decrease in the hardness of the pure Cu. Therefore, the hardness of Cu may vary depending on heat treatment. In the present study, Cu re-casting has a hardness of 74.54 HV.

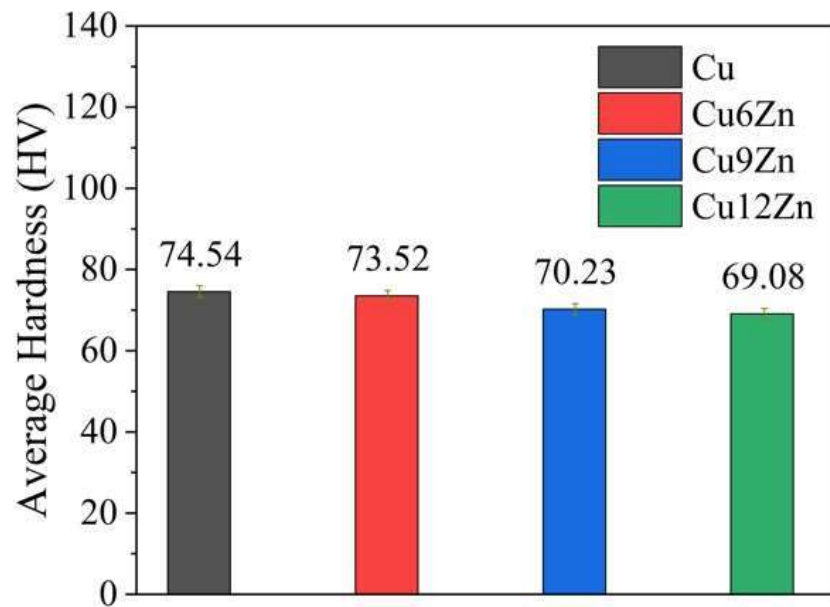


Fig. 2. Average hardness of various casting samples.

According to Figure 2, it can be seen that an increase in Zn content led to a decrease in the hardness. Another research study found that Cu (as-cast) has a hardness of around 100 HV, while Cu<sub>15</sub>Zn (as-cast) has a hardness of 75 HV (Ezequiel et al., 2024). Nnakwo et al. also found that increased Zn content in the Cu alloy leads to decreased hardness due to increased in grain size and solid solution

region (Nnakwo et al., 2021). According to a study by Qu et al. and García-Mintegui et al., pure Zn hardness is between 41-42 HV (García-Mintegui et al., 2021; Qu et al., 2020). Therefore, it could be concluded that Zn in the alloy leads to decreased hardness due to Zn hardness less than Cu.

Several researchers correlated measured hardness to crystallite size (Augustin et al., 2016; Syamsuir et al., 2023). Augustin et al. have found an increase in Cu's crystallite size, promoting a decrease in scratch and micro-hardness (Augustin et al., 2016). Syamsuir et al. found a decrease in Cu's crystallite size, leading to an increase in hardness (Syamsuir et al., 2023). Comparing Table 2 with Figure 2, it can be seen that an increase in the Zn content led to an increase in crystallite size and a decrease in the hardness. On the contrary, while as-cast samples do not form an alloy (Cu), the resulting hardness is not aligned with the crystallite size. It seems that it cannot compare the crystallite size were found with measured hardness between alloy (CuZn) and un-alloy (Cu) material.

Several transportation sectors, such as ambulance equipment, are made from Al alloy (Blanco et al., 2022; Vandersluis et al., 2020). According to Hajizadeh et al., Al alloy hardness is between 32-52 HV (Hajizadeh et al., 2017). Therefore, all specimens have hardness still higher than Al alloy.

#### 4.3 OCP

Figure 3 shows the OCP measurement result of various casting samples in 0.9 % NaCl at room temperature. Generally, increased Zn content in the alloy promoted more negative potential, which perfectly agrees with the Cocco et al. study (Cocco et al., 2016). Dridi et al. have found that  $E_{OCP}$  CuZn30 and CuZn39 are -0.578 and -0.604 V/MSE at 3 % NaCl, which means an increase in the Zn promoted to more negative potential (Dridi et al., 2020). Cu, Cu6Zn, Cu9Zn, and Cu12Zn samples have  $E_{OCP}$  potential at 1200 s measurement -0.014, -0.023, -0.027, and -0.032 V vs Ag/AgCl, respectively.

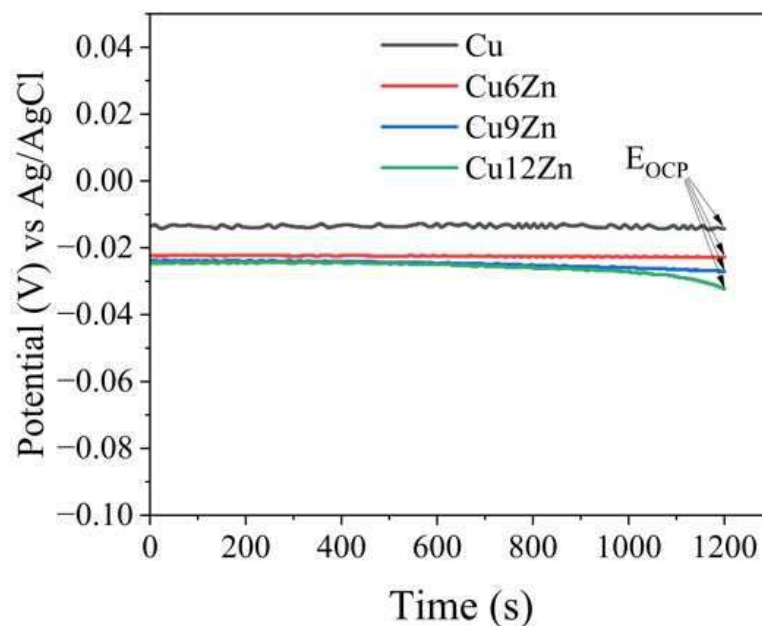


Fig. 3. OCP measurement of various casting samples.

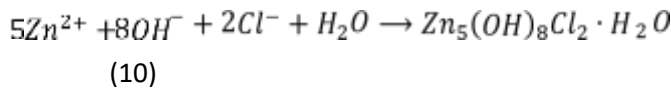
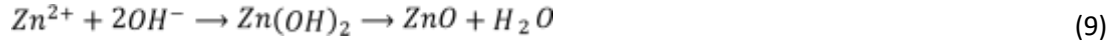
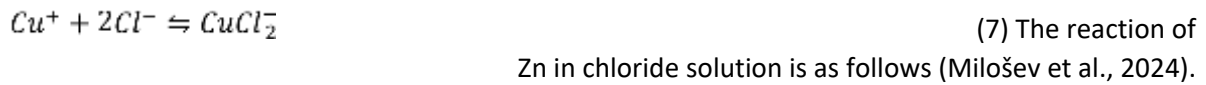
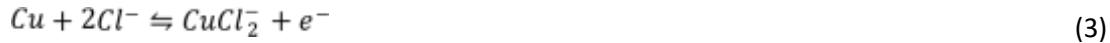
According to Figure 3, Cu, Cu6Zn, and Cu9Zn samples are steady at initial measurements until 1200 s, indicating that the protective layer formed has good protection. In contrast, the Cu12Zn sample is steady at initial measurements until 600 s, then moves in a more negative direction. These phenomena indicated that the formed protective layer had initially dissolved at 600 s; therefore, the measurement continuously moved forward in a negative direction until the measurement reached 1200 s.

#### 4.4 LSV

Eccrine sweat and saline-infused for humans are nearly 0.9 % of NaCl (Bond & Lieu, 2014; Tayyab et al., 2021). Therefore, LSV measurement was conducted in 0.9 % NaCl at room temperature. Luo et al. found Cu<sub>2</sub>O crystalline growth on the Cu surface when exposed to 0.9 % NaCl, while when exposed to pure water, Cu<sub>2</sub>O crystalline was not seen (Luo et al., 2020). Commonly, Cu<sub>2</sub>O crystallines are formed, which is preceded by the formation of CuCl when the specimen is tested in a chloride solution. Moreover, Zhang et al., in their study, found ZnO and

Zn<sub>5</sub>Cl<sub>2</sub>(OH)<sub>8</sub>·H<sub>2</sub>O as corrosion products on top of Cu40Zn surfaces in a chloride environment

(Zhang et al., 2016). The reaction of Cu in chloride solution is as follows (Milošev et al., 2024).



LSV measurement results in 0.9 % NaCl can be seen in Figure 4.

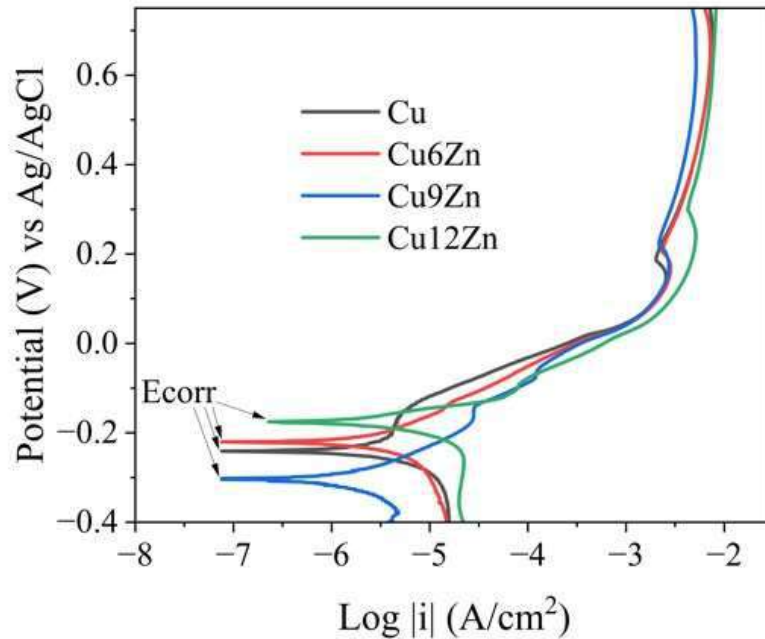


Fig. 4. LSV scans result of various casting samples.

According to Figure 4, corrosion  $E_{corr}$  and  $i_{corr}$  can be found using the Tafel extrapolation method. Moreover, the corrosion rate could be calculated by inserting  $i_{corr}$  into expression (1). Table 3 presented  $E_{corr}$ ,  $i_{corr}$ , and the corrosion rate of various casting samples. It appears  $E_{corr}$  is independent of Zn addition; however, Zn is dependent on  $i_{corr}$  and corrosion rate (except for the Cu12Zn sample). This behavior is probably due to a protective layer that was formed. Compared to the OCP result, it can be seen that the Cu12Zn sample continuously moves forward in a negative direction from 600 until 1200 s of measurement. Therefore, that sample has a higher  $i_{corr}$  and corrosion rate.

Table 3 - Corrosion parameters of various casting samples.

Sample name	$E_{corr}$ (V) vs Ag/AgCl	$i_{corr}$ (A/cm <sup>2</sup> )	Corrosion rate (mmpy)
Cu	-0.241	$4.42 \times 10^{-6}$	$5.13 \times 10^{-2}$
Cu6Zn	-0.220	$3.33 \times 10^{-6}$	$3.86 \times 10^{-2}$
Cu9Zn	-0.304	$2.15 \times 10^{-6}$	$2.49 \times 10^{-2}$
Cu12Zn	-0.175	$6.19 \times 10^{-6}$	$7.18 \times 10^{-2}$

Qu et al. have found that an increase in Zn content led to an increase in corrosion resistance, which perfectly agrees with the present study (except for Cu12Zn) (Qu et al., 2020). Milošev et al. investigated Cu, Cu10Zn, Cu40Zn, and Zn in 3 % NaCl and found  $i_{corr}$  after stabilized at 1 hour around 1.573, 1.456, and 2.114, and 5.21  $\mu\text{A}/\text{cm}^2$  respectively (Milošev et al., 2024). According to equation (1),  $i_{corr}$  strongly influences the corrosion rate. The more  $i_{corr}$ , the higher the corrosion rate. Moreover, a limitation in Zn content in the Cu alloy could influence the corrosion resistance. Presenting the Zn content  $\leq 11$  wt.% in the alloy could enhance the corrosion resistance; however, Zn of more than 10 wt.% could decrease corrosion resistance (Milošev et al., 2024).

According to Table 2, the Cu9Zn sample has the lowest microstrain than others. The measured microstrain could be associated with the sample's crystal defect (Soegijono et al., 2020). Based on Table 2, the Cu9Zn sample has the lowest microstrain, which confirms that the sample has the lowest



corrosion rate. Moreover, the FCC sample with the preferred orientation of the (111) plane could offer a lower corrosion rate due to the highest surface atomic density (Jinlong et al., 2016; Soegijono et al., 2020). Compared to other samples, the Cu9Zn sample has the higher preferred orientation of the (111) plane. Even though the (111) plane of the Cu sample is the highest. Unfortunately, the (220) and (200) planes are still present and relatively high.

#### 4.5 Antibacterial Activity

Figure 5 shows the direct contact kill of *Staphylococcus aureus* and *Escherichia coli* after 24 hours of incubation. The present study focused on *Staphylococcus aureus*, but *Escherichia coli* was also used for comparison. There is no diffusion in the sample; therefore, the inhibition zone could not be seen.

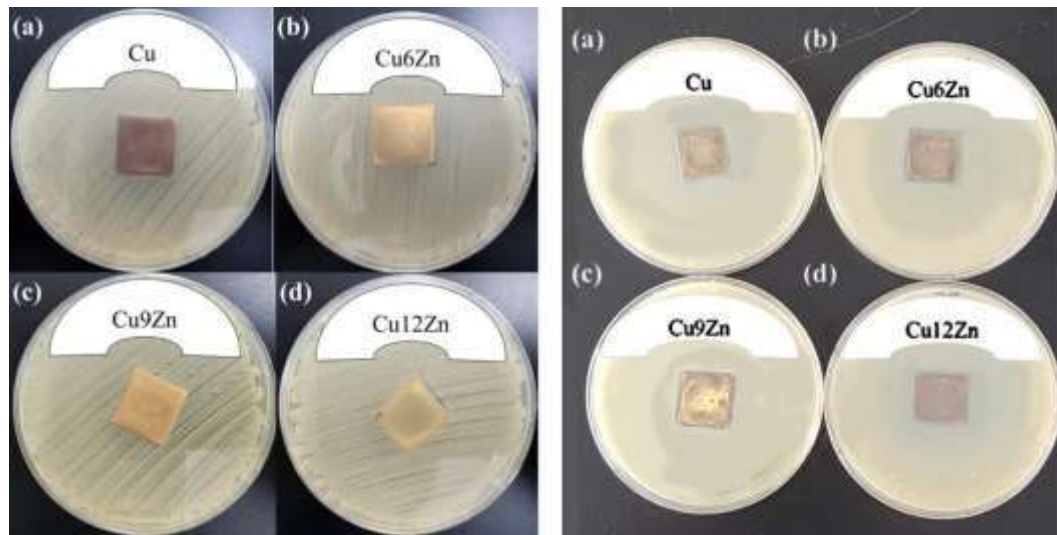


Fig. 5. Antibacterial activity test using *Staphylococcus aureus* (left) and *Escherichia coli* (right) (a) Cu, (b) Cu6Zn, (c) Cu9Zn, and (d) Cu12Zn.

Antibacterial activity after 24 hours of post-contact with various casting samples using *Staphylococcus aureus* and *Escherichia coli* can be seen in Figure 6. The removed sample places remain clear (with no regrowth) from bacterial activity. The antibacterial behavior was significantly influenced by Cu or Zn ions (Qu et al., 2020). Villapún et al. found that releasing Cu ions leads to the highest killing activity of *Staphylococcus aureus* (Villapún et al., 2016). Excess in the Cu ion could be bacteriostatic (Sabbouh et al., 2023). Moreover, Cu ions could be adsorbed on the cytoplasmic membrane surfaces, then penetrate the bacteria, react with sulfhydryl groups and cause the cell to die (Zeng et al., 2022). Furthermore, Cu ions could form hydroxyl groups in the presence of oxygen in nature, which could destroy cell membranes (Dou et al., 2022). Hutchings et al. stated that  $Zn^{2+}$  successfully inhibits the growth of *S. epidermidis* (Hutchings et al., 2021). This behavior is associated with the generation of reactive oxygen or the formation of (Zhang et al., 2021).

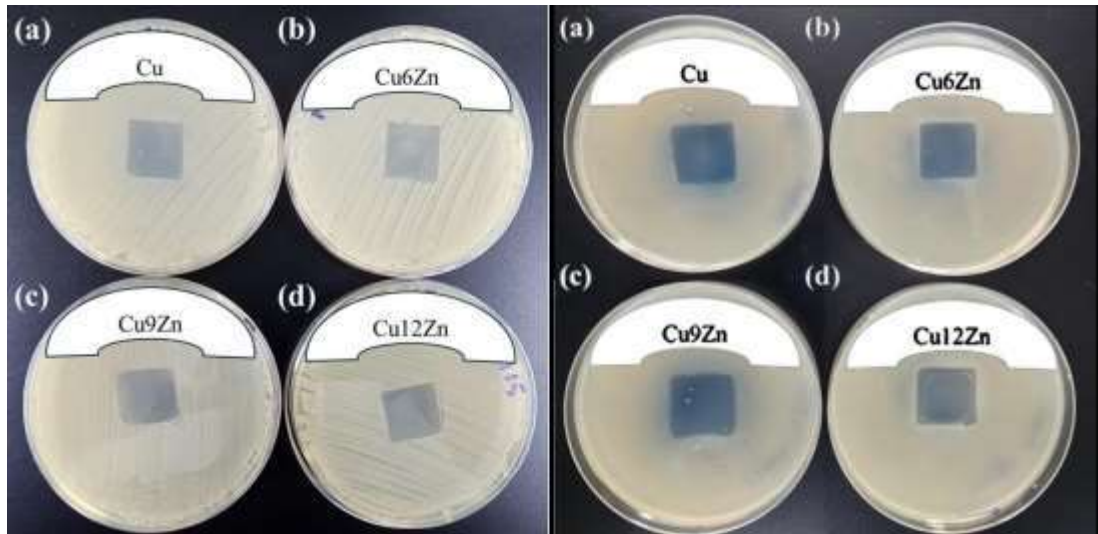


Fig. 6. Antibacterial activity after 24 hours of post-contact (regrowth assessment) towards *Staphylococcus aureus* (left) and *Escherichia coli* (right) (a) Cu, (b) Cu6Zn, (c) Cu9Zn, and (d) Cu12Zn

Figure 7 shows the fluid contact test of *Staphylococcus aureus* and *Escherichia coli*. The orientation of the test materials is mapped within the yellow box. For the Cu6Zn sample, *Escherichia coli* was killed on the 3<sup>rd</sup> hour. However, there is no significant reduction within the fluid because there are no diffusible materials. Also, there is no visible growth after 3<sup>rd</sup> hour for the fluid in contact with the metal.

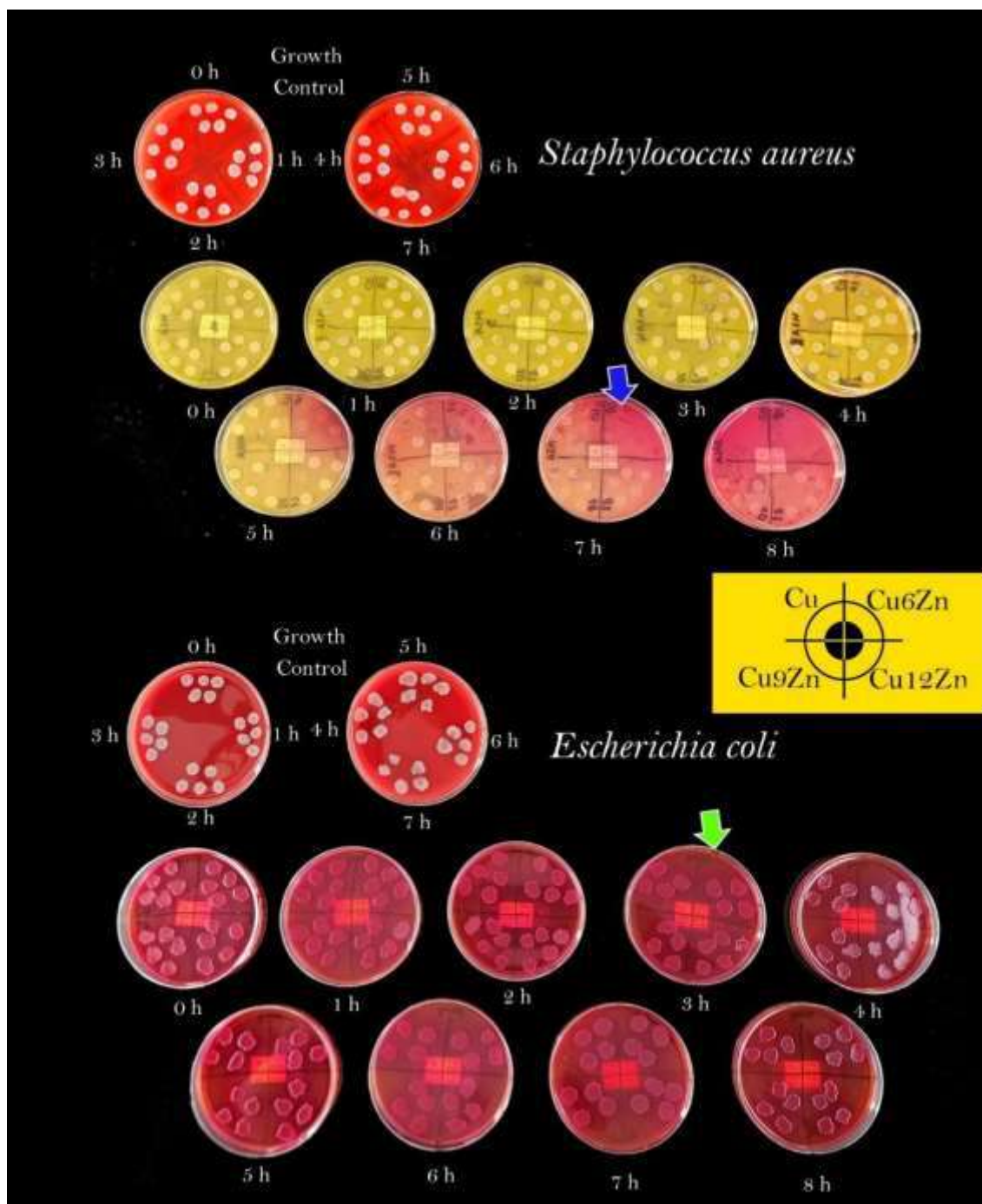


Fig. 7. Fluid contact test of *Staphylococcus aureus* and *Escherichia coli*

Moreover, it should be noted that the reduction of the colony is significant in the 7<sup>th</sup> hour for *Staphylococcus aureus* (blue arrow), but for *Escherichia coli*, the inhibition of *Escherichia coli* growth is shown within the 3<sup>rd</sup> hour of contact (green arrow), for Cu6Zn sample. The reduction of colonies is significant on the surface of the metal. While on the remaining fluid, the reduction is insignificant until 8 hours. This behavior is because *Staphylococcus aureus* and *Escherichia coli* have different membrane structures and thick cell walls, therefore could inhibit ion exchange and restrain the antibacterial effect of Cu and or Zn ions (Di et al., 2022). Cu killing is more effective in Gram-negative bacteria (e.g.,

*Escherichia coli*) because peptidoglycan affects the cell's susceptibility. The thicker the peptidoglycan layer, the harder it became for the Cu ions to reach the membrane (Soltani et al., 2020; Xhafa et al., 2023). Therefore, *Escherichia coli* was killed in the 3<sup>rd</sup> hour. Another reason Cu6Zn has better antibacterial performance than others is probably due to its smaller crystallite size. Researchers found that smaller crystallite sizes promote the enhancement of antibacterial effects (Syamsuir et al., 2023). This behavior is attributed to an increase in surface area due to the crystallite size (Sangeetha et al., 2015). The Cu6Zn sample could be used as an alternative material for medical equipment in ambulances.

## 5. Conclusion

CuZn has been successfully fabricated. XRD confirmed that CuZn alloy has a single alpha phase with an FCC crystal structure. The rise of the Zn content in the alloy led to a decrease in the hardness due to an increase in crystallite size and led to a shift to more negative OCP potential at 1200 s measurement. Moreover, the rise of the Zn content to 9 wt.% decreased the corrosion rate. It appears there is a limitation in Zn content in the copper alloy that influences the corrosion rate, as shown when Zn content around 12 wt. % is promoted to increase the corrosion rate. Antibacterial activity observation found that all samples had no diffusion. Moreover, 24-hour post-contact observation found that sample places removed from the sample remained clear of bacteria. The Cu6Zn has better antibacterial performance than others due to the smallest crystallite size. According to the fluid contact test, the reduction of the colony of *Staphylococcus aureus* is significant in the 7<sup>th</sup> hour. The inhibition of *Escherichia coli* growth is also shown within the 3<sup>rd</sup> hour of contact. This behavior is because *Staphylococcus aureus* and *Escherichia coli* have different membrane structures and thick cell walls, therefore, could inhibit ion exchange and restrain the antibacterial effect of Cu and or Zn ions.

## Acknowledgement

This research is under financial support from the Ministry of Education, Culture, Research and Technology Indonesia with contract number 832/LL3/AL.04/2024 and 171/A/LPPM-P/USAKTI/VI/2024.

## References

- Abed, K. M., & Dawood, N. M. (2022). Impacts of Tin and Germanium on Corrosion and Erosion-Corrosion Behavior of 60Cu-40Zn alloys. *AIP Conference Proceedings*, 2660, 020131. <https://doi.org/10.1063/5.0108474>
- Akhyar, Iqbal, Ali, N., & Husin, H. (2023). Effect of variations in pouring temperature on tensile strength of CuZn cast alloys. *Materials Letters: X*, 17, 100182. <https://doi.org/10.1016/j.mlblux.2023.100182>
- Augustin, A., Huilgol, P., Udupa, K. R., & Bhat K, U. (2016). Effect of current density during electrodeposition on microstructure and hardness of textured Cu coating in the application of antimicrobial Al touch surface. *Journal of the Mechanical Behavior of Biomedical Materials*, 63, 352–360. <https://doi.org/10.1016/j.jmbbm.2016.07.013>



- Azizian, F., Naffakh-Moosavy, H., & Bagheri, F. (2024). The role of Cu addition in the metallurgical features, mechanical properties, and cytocompatibility of cardiovascular stents biodegradable Zn-based alloy. *Intermetallics*, 164, 108106. <https://doi.org/10.1016/j.intermet.2023.108106>
- Baker, L. B., & Wolfe, A. S. (2020). Physiological mechanisms determining eccrine sweat composition. *European Journal of Applied Physiology*, 120(4), 719–752. <https://doi.org/10.1007/s00421-020-04323-7>
- Bhavsar, V., & Bali, S. C. (2023). Effect of Compressed Natural Gas (CNG) on corrosion behaviour of brass valve of CNG cylinder. *Engineering Failure Analysis*, 149, 107268. <https://doi.org/10.1016/j.engfailanal.2023.107268>
- Blanco, D., Mar, E., & Mar, R. (2022). Titanium Alloys Applied to the Transport Sector : A Review. *Metals*, 12(9), 1–21. <https://doi.org/10.3390/met12010009>
- Bond, J. W., & Lieu, E. (2014). Electrochemical behaviour of brass in chloride solution concentrations found in eccrine fingerprint sweat. *Applied Surface Science*, 313, 455– 461. <https://doi.org/10.1016/j.apsusc.2014.06.005>
- Chen, L., Ma, R., Dong, J., Chen, S., Li, C., Ma, C., Bian, G., & Wang, C. (2024). A multi-ion transport model of Cu-Zn-Fe trimetallic couple in near-neutral NaCl solution. *Corrosion Science*, 239, 112414. <https://doi.org/10.1016/j.corsci.2024.112414>
- Clement, A., & Auger, T. (2023). An EAM potential for  $\alpha$ -brass copper-zinc alloys: application to plasticity and fracture. *Modelling and Simulation in Materials Science and Engineering*, 31(1), 015004. <https://doi.org/10.1088/1361-651X/aca4ec>
- Cocco, F., Fantauzzi, M., Elsener, B., & Rossi, A. (2016). Dissolution of brass alloys naturally aged in neutral solutions-an electrochemical and surface analytical study. *RSC Advances*, 6(93), 90654–90665. <https://doi.org/10.1039/c6ra18200c>
- Di, T., Xu, Y., Liu, D., & Sun, X. (2022). Microstructure, Mechanical Performance and AntiBacterial Activity of Degradable Zn-Cu-Ag Alloy. *Metals*, 12(9), 1–13. <https://doi.org/10.3390/met12091444>
- Dou, X., Chen, Y., & Shi, H. (2022). CuBi<sub>2</sub>O<sub>4</sub>/BiOBr composites promoted PMS activation for the degradation of tetracycline: S-scheme mechanism boosted Cu<sup>2+</sup>/Cu<sup>+</sup> cycle. *Chemical Engineering Journal*, 431(P2), 134054. <https://doi.org/10.1016/j.cej.2021.134054>
- Dridi, A., Dhouibi, L., Hihn, J. Y., Berçot, P., Rezrazi, E. M., Sassi, W., & Rouge, N. (2020). Analytical Study of CuZn 30 and CuZn 39 Brass Surfaces in 3% NaCl Solution Under Polarization. *Chemistry Africa*, 3(3), 735–747. <https://doi.org/10.1007/s42250-02000182-z>

Du, M., Zhao, W., Ma, R., Xu, H., Zhu, Y., Shan, C., Liu, K., Zhuang, J., & Jiao, Z. (2021). Visible-light-driven photocatalytic inactivation of *S. aureus* in aqueous environment by hydrophilic zinc oxide (ZnO) nanoparticles based on the interfacial electron transfer in *S. aureus*/ZnO composites.

*Journal of Hazardous Materials*, 418, 126013 Contents.

<https://doi.org/10.1016/j.jhazmat.2021.126013>

Ezequiel, M., Proriot Serre, I., Auger, T., Hériré, E., Hadjem-Hamouche, Z., & Perriere, L. (2024). The liquid metal embrittlement of a reactive system at room temperature: brasses in contact with the liquid eutectic Ga-In. *Engineering Failure Analysis*, 164,

108694. <https://doi.org/10.1016/j.engfailanal.2024.108694>

Gao, P., Ren, Y., Qian, S., He, Y., & Shen, D. (2021). Evolution of microstructure and electrochemical corrosion behavior of CuZn-based alloys induced by cold rolling.

*Journal of Materials Research and Technology*, 15, 360–368.

<https://doi.org/10.1016/j.jmrt.2021.08.035>

García-Mintegui, C., Córdoba, L. C., Buxadera-Palomero, J., Marquina, A., Jiménez-Piqué, E., Ginebra, M. P., Cortina, J. L., & Pegueroles, M. (2021). Zn-Mg and Zn-Cu alloys for stenting applications: From nanoscale mechanical characterization to in vitro degradation and biocompatibility. *Bioactive Materials*, 6(12), 4430–4446.

<https://doi.org/10.1016/j.bioactmat.2021.04.015>

Hajizadeh, K., Ejtemaei, S., & Eghbali, B. (2017). Microstructure, hardness homogeneity, and tensile properties of 1050 aluminum processed by constrained groove pressing. *Applied*

*Physics A: Materials Science and Processing*, 123(8), 1–9.

<https://doi.org/10.1007/s00339-017-1123-y>

Heidarzadeh, A., Javidani, M., & St-Georges, L. (2022). Crystallographic Orientation

Relationship between  $\alpha$  and  $\beta$  Phases during Non-Equilibrium Heat Treatment of Cu-37 wt. % Zn Alloy. *Crystals*, 12(1), 97. <https://doi.org/10.3390/cryst12010097>

Hendrawan, C. N., Setyani, A., Pertiwi, D. R. K., & Sofyan, B. T. (2021). Effect of 9wt% Mn addition on cold rolling and annealing behaviour of Cu-31Zn alloy. *Materials Today: Proceedings*, 46, 3346–3351. <https://doi.org/10.1016/j.matpr.2020.11.476>

*Proceedings*, 46, 3346–3351. <https://doi.org/10.1016/j.matpr.2020.11.476>

Huang, S. J., Li, C., Feng, J. H., Selvaraju, S., & Subramani, M. (2024). Mechanical and Corrosion Tests for Magnesium–Zinc/Ti-6Al-4V Composites by Gravity Casting. *Materials*, 17(8), 1836.

<https://doi.org/10.3390/ma17081836>

Hutchings, C., Yair, Z. P., Reifen, R., & Shemesh, M. (2021). Antimicrobial effect of  $\text{Zn}^{2+}$  ions governs the microbial quality of donor human milk. *Foods*, 10(3), 1–12. <https://doi.org/10.3390/foods10030637>

Iqbal, Ali, N., Husin, H., Akhyar, Khairil, & Farhan, A. (2021). Differences in Pour Temperature Affect Hardness Properties of CuZn Brass Alloy through Metal Casting. *IOP Conference Series: Materials Science and Engineering*, 1082(1), 012001. <https://doi.org/10.1088/1757-899x/1082/1/012001>

Jinlong, L., Tongxiang, L., & Chen, W. (2016). Effect of electrodeposition temperature on grain orientation and corrosion resistance of nanocrystalline pure nickel. *Journal of Solid State Chemistry*, 240, 109–114. <https://doi.org/10.1016/j.jssc.2016.05.025>

Karahan, I. H., & Özdemir, R. (2014). Effect of Cu concentration on the formation of Cu 1-x Zn x shape memory alloy thin films. *Applied Surface Science*, 318, 100–104. <https://doi.org/10.1016/j.apsusc.2014.01.119>

Liu, P., Hu, J. ying, Li, H. xue, Sun, S. yu, & Zhang, Y. bin. (2020). Effect of heat treatment on microstructure, hardness and corrosion resistance of 7075 Al alloys fabricated by SLM. *Journal of Manufacturing Processes*, 60, 578–585. <https://doi.org/10.1016/j.jmapro.2020.10.071>

Luo, J., Hein, C., Pierson, J. F., & Mücklich, F. (2020). Sodium chloride assists copper release, enhances antibacterial efficiency, and introduces atmospheric corrosion on copper surface. *Surfaces and Interfaces*, 20, 100630. <https://doi.org/10.1016/j.surfin.2020.100630>

Milošev, I., Taheri, P., Kapun, B., Kozlica, D. K., Mol, A., & Kokalj, A. (2024). The effect of molecular structure of imidazole-based compounds on corrosion inhibition of Cu, Zn, and Cu-Zn alloys. *Corrosion Science*, 127870. <https://doi.org/10.1016/j.corsci.2024.112328>

Morath, L., Rahim, S. A., Baker, C., Anderson, D., Hinds, M., Sikora-Jasinska, M., Oujiri, L., Leyssens, L., Kerckhofs, G., Pyka, G., Oliver, A. A., Drelich, J. W., & Goldman, J. (2024). The biological effects of copper alloying in Zn-based biodegradable arterial implants. *Biomaterials Advances*, November, 124658. <https://doi.org/10.1016/j.bioadv.2024.214112>

Mousavi, S. E., Sonboli, A., Naghshehkish, N., Meratian, M., Salehi, A., & Sanayei, M. (2020). Different behavior of alpha and beta phases in a Low Stacking Fault Energy copper alloy under severe plastic deformation. *Materials Science and Engineering: A*, 788, 139550. <https://doi.org/10.1016/j.msea.2020.139550>

Nikhil, Singh, M. K., Ji, G., & Prakash, R. (2021). Investigation on the effects of cooling rate on surface Texture, corrosion behaviour and hardness of pure copper. *Materials Today: Proceedings*, 47(19), 6693–6695. <https://doi.org/10.1016/j.matpr.2021.05.115>

Nnakwo, K. C., Osakwe, F. O., Ugwuanyi, B. C., Oghenekowho, P. A., Okeke, I. U., & Maduka, E. A. (2021). Grain characteristics, electrical conductivity, and hardness of Zndoped Cu–3Si alloys system. *SN Applied Sciences*, 3(11), 829. <https://doi.org/10.1007/s42452-021-04784-1>

Nuryadi, N., Sudarsono, B., & Asistyasari, A. (2020). Effect of Moisture Content of Green Sand on The Casting Defects. *Journal of Applied Engineering and Technological Science*, 4(1), 586–598.

Özdemir, R., & Karahan, I. H. (2014). Electrodeposition and properties of Zn, Cu, and Cu 1-x

Zn x thin films. *Applied Surface Science*, 318, 314–318. <https://doi.org/10.1016/j.apsusc.2014.06.188>

Pietrocola, G., Campoccia, D., Motta, C., Montanaro, L., Arciola, C. R., & Speziale, P. (2022). Colonization and Infection of Indwelling Medical Devices by *Staphylococcus aureus* with an Emphasis on Orthopedic Implants. *International Journal of Molecular Sciences*, 23(11), 5958. <https://doi.org/10.3390/ijms23115958>

Qu, X., Yang, H., Jia, B., Yu, Z., Zheng, Y., & Dai, K. (2020). Biodegradable Zn–Cu alloys show antibacterial activity against MRSA bone infection by inhibiting pathogen adhesion and biofilm formation. *Acta Biomaterialia*, 117, 400–417. <https://doi.org/10.1016/j.actbio.2020.09.041>

Riaz, M., Najam, M., Imtiaz, H., Bashir, F., & Hussain, T. (2024). Structural and biological analysis of Zn–Cu based biodegradable alloys for orthopedic application. *Materials*

*Chemistry and Physics*, 312, 128618. <https://doi.org/10.1016/j.matchemphys.2023.128618>

Sabbouh, M., Nikitina, A., Rogacheva, E., Nebalueva, A., Shilovskikh, V., Sadovnichii, R., Koroleva, A., Nikolaev, K., Kraeva, L., Ulasevich, S., & Skorb, E. (2023). Sonochemical fabrication of gradient antibacterial materials based on Cu-Zn alloy. *Ultrasonics Sonochemistry*, 92, 106247. <https://doi.org/10.1016/j.ultsonch.2022.106247>

Sangeetha, R., Muthukumaran, S., & Ashokkumar, M. (2015). Structural, optical, dielectric and antibacterial studies of Mn doped Zn<sub>0.96</sub>Cu<sub>0.04</sub>O nanoparticles. *Spectrochimica Acta -*

*Part A: Molecular and Biomolecular Spectroscopy*, 144, 1–7. <https://doi.org/10.1016/j.saa.2015.02.056>

Shahriyari, F., Shaeri, M. H., Dashti, A., Zarei, Z., Noghani, M. T., Cho, J. H., & Djavanroodi, F. (2022). Evolution of mechanical properties, microstructure and texture and of various brass alloys processed by multi-directional forging. *Materials Science and Engineering: A*, 831, 142149. <https://doi.org/10.1016/j.msea.2021.142149>

Situmorang, E. M. H., Henniuriyama, V., & Soegijono, B. (2019). Oligodynamic Cu-Zn composite fabricated by powder metallurgy method. *Journal of Physics: Conference*

*Series*, 1191(1). <https://doi.org/10.1088/1742-6596/1191/1/012044>

- Soegijono, B., Susetyo, F. B., Yusmaniar, & Fajrah, M. C. (2020). Electrodeposition of paramagnetic copper film under magnetic field on paramagnetic aluminum alloy substrates. *E-Journal of Surface Science and Nanotechnology*, 18, 281–288. <https://doi.org/10.1380/EJSSNT.2020.281>
- Soltani, S., Akhbari, K., & White, J. (2020). Synthesis, crystal structure, magnetic, photoluminescence and antibacterial properties of dinuclear Copper(II) complex. *Journal of Molecular Structure*, 1214, 128233. <https://doi.org/10.1016/j.molstruc.2020.128233>
- Strzępek, P., Mamala, A., Zasadzińska, M., Franczak, K., & Jurkiewicz, B. (2019). Research on the drawing process of Cu and CuZn wires obtained in the cryogenic conditions. *Cryogenics*, 100, 11–17. <https://doi.org/10.1016/j.cryogenics.2019.03.007>
- Syamsuir, Susetyo, F. B., Soegijono, B., Yudianto, S. D., Basori, Ajiriyanto, M. K., Edbert, D., Situmorang, E. U. M., Nanto, D., & Rosyidan, C. (2023). Rotating-Magnetic-Field-Assisted Electrodeposition of Copper for Ambulance Medical Equipment. *Automotive Experiences*, 6(2), 290–302. <https://doi.org/10.31603/ae.9067>
- Tajik, S., Najar-Peerayeh, S., & Bakhshi, B. (2020). Hospital clones of Panton-Valentine leukocidin-positive and methicillin-resistant *Staphylococcus aureus* circulating in the Tehran community. *Journal of Global Antimicrobial Resistance*, 22, 177–181. <https://doi.org/10.1016/j.jgar.2019.12.010>
- Tayyab, K. Bin, Farooq, A., Alvi, A. A., Nadeem, A. B., & Deen, K. M. (2021). Corrosion behavior of cold-rolled and post heat-treated 316L stainless steel in 0.9wt% NaCl solution. *International Journal of Minerals, Metallurgy and Materials*, 28(3), 440–449. <https://doi.org/10.1007/s12613-020-2054-8>
- Vandersluis, E., Machin, A., Perovic, D., & Ravindran, C. (2020). Failure Analysis of an Ambulance Cathode Ray Tube Monitor Bracket. *Journal of Failure Analysis and Prevention*, 20(1), 23–33. <https://doi.org/10.1007/s11668-020-00804-1>
- Viegas, C., Sousa, P., Dias, M., Caetano, L. A., Ribeiro, E., Carolino, E., Twarużek, M., Kosicki, R., & Viegas, S. (2021). Bioburden contamination and *Staphylococcus aureus* colonization associated with firefighter's ambulances. *Environmental Research*, 197, 111125. <https://doi.org/10.1016/j.envres.2021.111125>
- Villapún, V. M., Dover, L. G., Cross, A., & González, S. (2016). Antibacterial metallic touch surfaces. *Materials*, 9(9), 1–23. <https://doi.org/10.3390/ma9090736>
- Wang, X., Su, H., Xie, Y., Wang, J., Feng, C., Li, D., & Wu, T. (2023). Atmospheric corrosion of T2 copper and H62 brass exposed in an urban environment. *Materials Chemistry and Physics*, 299, 127487. <https://doi.org/10.1016/j.matchemphys.2023.127487>

Widyastuti, Rochiem, R., Fellicia, D. M., Adrinanda, C. F. N., & Wibowo, A. P. (2023). Mechanical Properties, Microstructural, and Deep Drawing Formability Analysis on the Annealed CuZn35 Brass Alloy for Cartridge Application. *Key Engineering Materials*, 939, 31–37. <https://doi.org/10.4028/p-21x8y5>

Khafa, S., Olivieri, L., Di Nicola, C., Pettinari, R., Pettinari, C., Tombesi, A., & Marchetti, F. (2023). Copper and Zinc Metal–Organic Frameworks with Bipyrazole Linkers Display Strong Antibacterial Activity against Both Gram+ and Gram– Bacterial Strains. *Molecules*, 28(16), 6160. <https://doi.org/10.3390/molecules28166160>

Yin, M. yang, Li, Z., Xiao, Z., Pang, Y., Li, Y. ping, & Shen, Z. yan. (2021). Corrosion behavior of Cu–Al–Mn–Zn–Zr shape memory alloy in NaCl solution. *Transactions of Nonferrous Metals Society of China (English Edition)*, 31(4), 1012–1022.

[https://doi.org/10.1016/S1003-6326\(21\)65557-7](https://doi.org/10.1016/S1003-6326(21)65557-7)

Zeng, J., Geng, X., Tang, Y., Xiong, Z. C., Zhu, Y. J., & Chen, X. (2022). Flexible photothermal biopaper comprising Cu<sup>2+</sup>-doped ultralong hydroxyapatite nanowires and black phosphorus nanosheets for accelerated healing of infected wound. *Chemical Engineering Journal*, 437, 135347. <https://doi.org/10.1016/j.cej.2022.135347>

Zhang, E., Zhao, X., Hu, J., Wang, R., Fu, S., & Qin, G. (2021). Antibacterial metals and alloys for potential biomedical implants. *Bioactive Materials*, 6(8), 2569–2612. <https://doi.org/10.1016/j.bioactmat.2021.01.030>

Zhang, X., Liu, X., Odnevall Wallinder, I., & Leygraf, C. (2016). The protective role of hydrozincite during initial corrosion of a Cu<sub>40</sub>Zn alloy in chloride-containing laboratory atmosphere. *Corrosion Science*, 103, 20–29. <https://doi.org/10.1016/j.corsci.2015.10.027>

Ziat, Y., Hammi, M., Laghlimi, C., & Moutcine, A. (2020). Investment casting of leaded brass: Microstructure micro-hardness and corrosion protection by epoxy coating. *Materialia*, 12, 100794. <https://doi.org/10.1016/j.mtla.2020.100794>





# EFFECT OF ZINC ADDITION IN COPPER TO STRUCTURE, HARDNESS, CORROSION, AND ANTIBACTERIAL ACTIVITY

*by* Lisa Samura FTKE

---

**Submission date:** 03-Dec-2024 08:05PM (UTC+0700)

**Submission ID:** 2252552734

**File name:** JAETS\_Lisa\_Samura\_Rev\_19\_11\_2024.pdf (1.26M)

**Word count:** 6908

**Character count:** 36767

## **EFFECT OF ZINC ADDITION IN COPPER TO STRUCTURE, HARDNESS, CORROSION, AND ANTIBACTERIAL ACTIVITY**

**Lisa Samura<sup>1\*</sup>, Mustamina Maulani<sup>1</sup>, Cahaya Rosyidan<sup>1</sup>, Kartika Fajarwati Hartono<sup>1</sup>,  
Suryo Prakoso<sup>1</sup>, Evi Ulina Margareta Situmorang<sup>2</sup>, Daniel Edbert<sup>3</sup>, Bambang Soegijono<sup>4</sup>,  
Muhammad Yunan Hasbi<sup>5</sup>, Ferry Budhi Susetyo<sup>6</sup>**

Department of Petroleum Engineering, Universitas Trisakti, 11440, Indonesia<sup>1</sup>

Department of Physiology School of Medicine and Health Sciences, Atma Jaya Catholic  
University of Indonesia, 14440, Indonesia<sup>2</sup>

Department of Microbiology, Atma Jaya Catholic University of Indonesia, 14440, Indonesia<sup>3</sup>

PROUDTEK Lab., Department of Geoscience, Universitas Indonesia, 16424, Indonesia<sup>4</sup>

Research Center for Metallurgy – National Research and Innovation Agency, 15314, Indonesia<sup>5</sup>

Department of Mechanical Engineering, Universitas Negeri Jakarta, 13220, Indonesia<sup>6</sup>  
lisa.samura@trisakti.ac.id

*\*Corresponding Author*

### **ABSTRACT**

Brass (CuZn) is widely used today due to better mechanical, thermal, and chemical properties. The present research fabricated CuZn alloy by adding various Zn (6, 9, and 12 wt.%) to the Cu using gravity casting. Casts CuZn alloy by adding various Zn to the Cu to investigate optimum composition were resulting highest inhibited of bacterial activity. In addition, the structure, hardness, and electrochemical behavior of the alloy were also investigated using XRD, Vickers hardness, and potentiostat equipment. XRD confirmed that CuZn alloy has an alpha phase, and a FCC crystal structure. The rise of the Zn content in the alloy led to an increase in crystallite size, a decrease in the hardness and a shift to a more negative OCP potential at 1200 s measurement. Enhancing the Zn content to 9 wt.% in the alloy lead to decrease the corrosion rate. Moreover, 24-hour post-contact observation found that the sample places removed remained clear of bacteria. The Cu6Zn sample successfully inhibited the growth of *Escherichia coli* in the 3<sup>rd</sup> hour, while *Staphylococcus aureus* was 100 % reduced in the 7<sup>th</sup> hour. The Cu6Zn sample could be used as an alternative material for medical equipment in ambulances.

**Keywords :** XRD, Vickers, Electrochemical measurement, *Staphylococcus aureus*, *Escherichia coli*

### **1. Introduction**

Brass (CuZn) is an alloy widely used in the national defense, oil and gas industries, and health because it has better mechanical properties, thermal conductivity, and corrosion resistance (Bhavsar & Bali, 2023; Wang et al., 2023; Widyastuti et al., 2023). CuZn alloys for medical equipment in transportation such as ambulances need to consider two parameters: corrosion resistance and antibacterial characteristics. Commonly NaCl media was used to investigate corrosion for ambulance equipment. This condition due to ambulance equipment commonly exposure from medical patients eccrine sweat and saline-infused (Baker & Wolfe, 2020; Tayyab et al., 2021). Furthermore, some studies found that after cleaning the ambulance, 35.37 % of bacterial contaminants were still seen (Syamsuir et al., 2023).

Viegas et al. found *Staphylococcus aureus* was detectable on firefighter's ambulance equipment (Viegas et al., 2021). *Staphylococcus aureus* is a type of bacteria that could cause skin disease and is hard to treat with traditional antibiotics. *Staphylococcus aureus* bacteria tend to have methicillin resistance. According to Tajik et al., 38.4 % of *Staphylococcus aureus* methicillin resistant was found in Tehran community (Tajik et al., 2020). Moreover, this bacteria also could contaminate orthopedic implants and cause serious infections (Pietrocola et al., 2022).

Several researchers were interested in investigating the corrosion behavior of CuZn alloy in NaCl medium (Abed & Dawood, 2022; Chen et al., 2024; Gao et al., 2021; Yin et al., 2021). Abed and Dawood investigated the corrosion behavior of Cu40Zn alloy in 3.5% NaCl and found a corrosion rate of around 0.037 mmpy (Abed & Dawood, 2022). Yin et al. investigated the corrosion behavior of Cu alloy in NaCl medium were immersed in different times. More time is immersed, resulting in more corrosion resistance of Cu (Yin et al., 2021). Chen et al. investigated Cu alloy in NaCl medium and found Cu potential around -0.305 V vs SCE and Zn potential around -1.165 V vs SCE (Chen et al., 2024). Gao et al. found that a reduction in thickness (50 to 60 %) of CuZn using cold rolling resulted in a significant decrease in corrosion current from 4.824 to 1.804  $\mu\text{A}/\text{cm}^2$  (investigating in 3.5 % NaCl) (Gao et al., 2021). Moreover, aluminum (Al) alloy widely used in transportation sector such as ambulance (Blanco et al., 2022; Vandersluis et al., 2020). Liu et al. have found Al alloy corrosion current between 4.868-5.251  $\text{A}/\text{cm}^2$  in a 3.5% NaCl medium (Liu et al., 2020). Comparing the studies of Liu et al. and Gao et al., Al alloy has a higher corrosion current than CuZn (Gao et al., 2021; Liu et al., 2020). Corrosion current significantly influences the corrosion rate, and a rise in the corrosion current would enhance the corrosion rate.

Recently, researchers have been interested in investigating CuZn alloy for medical applications (Azizian et al., 2024; Riaz et al., 2024; Sabbouh et al., 2023). Azizian et al. investigated CuZn alloys microstructure, mechanical properties and cytotoxicity for cardiovascular applications (Azizian et al., 2024). Riaz et al. investigated the structural and biological properties of CuZn alloy for orthopedic applications (Riaz et al., 2024). Moreover, Sabbouh et al. did the sonification of CuZn in an alkali solution to enhance the antibacterial inhibition zone (Sabbouh et al., 2023). Moreover, Syamsuir et al. have investigated the antibacterial activity of *Staphylococcus aureus* by presenting a Cu layer for ambulance equipment (Syamsuir et al., 2023).

The killing mechanism of bacterial activity inseparable from the ions released by the alloy (Qu et al., 2020).  $\text{Cu}^{2+}$  ions could be adsorbed on the cytoplasmic membrane surfaces, then penetrate the bacteria, react with sulfhydryl groups, and cause the cell to die (Zeng et al., 2022). The released  $\text{Zn}^{2+}$  ions could penetrate the cell membrane and cause cell death (Du et al., 2021). Zhang et al. have stated that  $\text{Cu}^{2+}$  and  $\text{Zn}^{2+}$  ions could act as antibacterial agents and inhibit *Staphylococcus aureus* growth (Zhang et al., 2021).

According to the literature review, research on CuZn alloys with Zn compositions in the range of 6–12 wt.% for medical transportation purposes has not been thoroughly investigated. As mentioned above, the killing mechanism of bacterial activity depend on Cu and Zn ions. CuZn alloy can transform into Cu and Zn ions. Therefore, the present research casts CuZn alloy by adding various Zn to the Cu to investigate optimum composition, resulting in a higher killing mechanism of bacterial activity. Moreover, different alloy compositions would result in different electrochemical behavior and mechanical properties. The present study investigated structure, hardness, electrochemical behavior, and antibacterial activity using X-ray diffraction (XRD), Vickers hardness equipment, potentiostat, and digital camera.

## 2. Literature Review

Many techniques are used to make CuZn alloys, including gravity and investment casting (Hendrawan et al., 2021; Ziat et al., 2020). Gravity casting is simple, inexpensive, and can rapidly fill complex geometry (Huang et al., 2024; Nuryadi et al., 2020). Moreover, in the fabrication of CuZn alloys, one thing needs to be considered to produce specific properties, namely alloy composition. Researchers focused on adding various Zn compositions onto Cu for different purposes. Strzpek et al. investigated the mechanical properties of Cu and alpha brass (Cu2.5Zn and Cu6.5Zn) wire ( $\varnothing$  3.8 mm). Increased Zn content causes increases in ultimate tensile strength, yield strength and hardness (Strzpek et al., 2019). Situmorang et al. fabricated Cu with various Zn additions (10, 20, 38, and 45 wt.%) and found that the higher the Zn composition, the higher the antibacterial properties (Situmorang et al., 2019). Iqbal et al. melted Cu28.7Zn using a furnace and cast to investigate hardness and morphology (Iqbal et al., 2021). Shahriyari et al. added Zn (5, 15, 20, and 30 wt.%), increasing the hardness due to the alloy's rise in the Zn content

(Shahriyari et al., 2022). Akhyar et al. melted Cu<sub>28.7</sub>Zn using a gas furnace and cast to investigate the tensile strength (Akhyar et al., 2023). Morath et al. have created Zn<sub>0.8</sub>Cu and Zn<sub>1.5</sub>Cu using casting methods to investigate the biological aspect of arterial implants (Morath et al., 2024). Azizian et al. have added Cu with compositions 1, 2, and 5 wt.% to CuZn alloy by melting in the induction furnace to investigate microstructure, mechanical properties, and cytotoxicity for cardiovascular application (Azizian et al., 2024). Generally, a CuZn alloy with a Zn composition of less than 37 wt.% would produce a single alpha phase with an FCC crystal structure (Clement & Auger, 2023; Mousavi et al., 2020).

### 3. Research Methods

#### 3.1 Material Preparation

Cu ingot (98.798 %) and Zn powder (99 %) were melted and cast with the alloy composition Cu<sub>x</sub>Zn (x=0, 6, 9, and 12 wt.%, namely as Cu, Cu<sub>6</sub>Zn, Cu<sub>9</sub>Zn, and Cu<sub>12</sub>Zn, respectively) and then confirmed the formed alloy using XRF (Table 1). Before melting was conducted, the ingot and the apparatus, such as the crucible, were cleaned using water to avoid impurities and then dried. The Cu ingot was first filled into a silicon carbide crucible (3kg) and then inserted into a muffle furnace. Melting was carried out in a crucible at 1100 °C under atmospheric pressure. After the Cu has melted, remove it from the muffle furnace, mix it with Zn powder, stir it manually, and pour it into a permanent mold. For comparison, Cu ingot was melted and poured into a permanent mold without Zn addition. The as-cast ingots were cut for further characterization, such as XRD, hardness, electrochemical measurement, and antibacterial activity observation.

Table 1 – Chemical composition of various casting samples.

Sample	Element (wt.%)					
	Cu	Zn	Al	Si	P	Fe
Cu	98.798	-	0.135	0.444	0.384	0.238
Cu <sub>6</sub> Zn	92.308	6.384	0.135	0.444	0.384	0.345
Cu <sub>9</sub> Zn	89.228	9.497	0.135	0.444	0.384	0.312
Cu <sub>12</sub> Zn	87.075	11.557	0.135	0.444	0.384	0.405

#### 3.2 XRD Measurement

XRD was measured using the PANalytical (Cu K $\alpha$ 1  $\lambda$ =1.5405980) apparatus. XRD was scanned from 20 to 100°, using step size 0.0217°. The Highscore software was used to refine and collect peak, phase and crystallographic parameters of as-cast samples. By using that software, full width at half maximum (FWHM) are also found. FWHM data is used to calculate crystallite size.

#### 3.3 Hardness Measurement

Before testing, samples with 20×20×6 mm dimensions were polished using silicon carbide up to #3000 grit. Afterward, the polished sample was cleaned using water, followed by alcohol, and then dried using drier equipment. The hardness test was conducted using the Vickers method. An FV-300e hardness test was performed on top of various samples using 1 kg of load. Ten repeatable measurements were conducted.

#### 3.4. Electrochemical Measurement

Two electrochemical measurements were conducted in the present research, such as open circuit potential (OCP) and Linear sweep voltammetry (LSV), using Digi-Ivy (DY2311) potentiostat in 0.9 % NaCl at room temperature. OCP was scanned until 1200 s using a sampling scan rate of 0.02 s, while LSV was conducted using a scan rate of 1 mV/s. Cu/CuZn samples are used as the working electrode, platinum wire as the counter electrode, and Ag/AgCl as the reference electrode. LSV data was examined using the Tafel extrapolation method to see corrosion potential ( $E_{corr}$ ) and current density ( $i_{corr}$ ). The corrosion rate could be found by inserting  $i_{corr}$  in the following equation (Soegijono et al., 2020).

$$\text{Corrosion rate (mmpy)} = C \frac{M \times i_{\text{corr}}}{\rho \times n} \quad (1)$$

Where C is corrosion constant (3.27 mmpy), M is atomic weight (g/mol),  $\rho$  is material density (g/cm<sup>3</sup>), and n is the number of electrons involved.

### 3.5 Antibacterial Activity Observation

The sample dimension used for antibacterial activity is 20×20×6 mm. Before testing, samples were polished using silicon carbide up to #3000 grit. The experimental procedure for antibacterial activity is similar to that of the previous report (Syamsuir et al., 2023). Moreover, the recent study uses *Staphylococcus aureus* ATCC 25923 for Direct contact kill assay (24 hours) and Fluid contact assay (8 hours). In comparison, *Escherichia coli* 25922 was also used in the present study. Afterward, documentation was captured using a digital camera. In addition, 24-hour post-contact observation and Fluid contact test were also captured using a digital camera.

## 4. Results and Discussions

### 4.1 XRD

The diffraction pattern of Cu/CuZn with (111), (200), (311), and (222) planes can be seen in Figure 1. The four diffraction patterns match the alpha phase, which is shown to align with another study (Heidarzadeh et al., 2022). The acquired XRD data was then analyzed using Highscore software, and the parameters are listed in Table 2. All samples had a face-centered cubic (FCC) crystal structure, indicating that the Cu and Zn atoms dissolve into one another. According to Jinlong et al., the FCC quantity of surface energy is (111)>(001)>(110), and the FCC sample with the (111) plane has the lowest corrosion rate (Jinlong et al., 2016). Moreover, the FCC sample with the preferred orientation of the (111) plane has the highest surface atomic density (Soegijono et al., 2020).

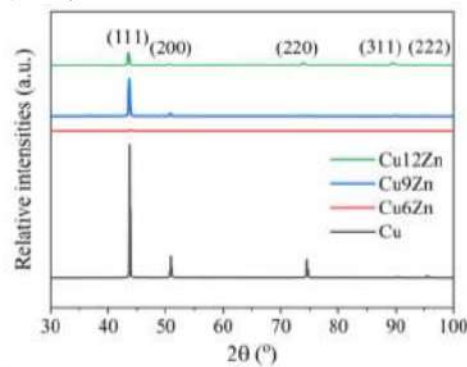


Fig. 1. XRD of various casting samples.

Table 2 - Crystallographic parameters of various casting samples.

Parameter	Sample			
	Cu	Cu6Zn	Cu9Zn	Cu12Zn
Crystal structure	FCC			
Lattice constant $a = b = c$ (Å)	2.964	8.929	2.981	2.964
Cell volume (Å <sup>3</sup> )	26.03	90	26.49	26.05
d-spacing (Å)	1.69	1.18	1.69	2.07
Crystallite Size (nm)	227.20	109.95	204.95	316.26
Micro strain	0.37	0.53	0.16	0.32

Presenting Zn in the alloy reduces crystallite size from 227.20 to 109.95 nm and increases Zn content from 6 to 12 wt.%, leading to an increase in crystallite size from 109.95 to 316.26 nm.



This behavior is similar to Özdemir and Karahan's study that showed Zn in the alloy leads to decreased crystallite size, and an increase in Zn content in the alloy leads to increased crystallite size (Özdemir & Karahan, 2014). Moreover, the microstrains of the as-cast sample are independent of Zn content, which perfectly agrees with Karahan and Özdemir's study ((Karahan & Özdemir, 2014). The smallest microstrain is seen in the Cu9Zn sample.

#### 4.2 Hardness

Figure 2 shows the average hardness of various casting samples. Nikhil et al. have found that pure Cu has a hardness of 140 HV when treated at 400 and 600 °C and then held for two hours, followed by quenching in tap water, resulting in a hardness of 100 and 60 HV (Nikhil et al., 2021). The higher heat treatment temperatures led to a decrease in the hardness of the pure Cu. Therefore, the hardness of Cu may vary depending on heat treatment. In the present study, Cu re-casting has a hardness of 74.54 HV.

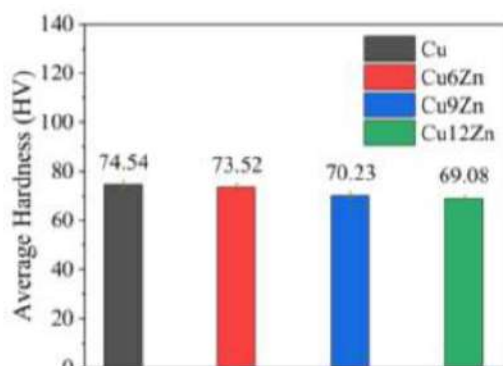


Fig. 2. Average hardness of various casting samples.

According to Figure 2, it can be seen that an increase in Zn content led to a decrease in the hardness. Another research study found that Cu (as-cast) has a hardness of around 100 HV, while Cu15 Zn (as-cast) has a hardness of 75 HV (Ezequiel et al., 2024). Nnakwo et al. also found that increased Zn content in the Cu alloy leads to decreased hardness due to increased in grain size and solid solution region (Nnakwo et al., 2021). According to a study by Qu et al. and García-Mintegui et al., pure Zn hardness is between 41–42 HV (García-Mintegui et al., 2021; Qu et al., 2020). Therefore, it could be concluded that Zn in the alloy leads to decreased hardness due to Zn hardness less than Cu.

Several researchers correlated measured hardness to crystallite size (Augustin et al., 2016; Syamsuir et al., 2023). Augustin et al. have found an increase in Cu's crystallite size, promoting a decrease in scratch and micro-hardness (Augustin et al., 2016). Syamsuir et al. found a decrease in Cu's crystallite size, leading to an increase in hardness (Syamsuir et al., 2023). Comparing Table 2 with Figure 2, it can be seen that an increase in the Zn content led to an increase in crystallite size and a decrease in the hardness. On the contrary, while as-cast samples do not form an alloy (Cu), the resulting hardness is not aligned with the crystallite size. It seems that it cannot compare the crystallite size were found with measured hardness between alloy (CuZn) and un-alloy (Cu) material.

Several transportation sectors, such as ambulance equipment, are made from Al alloy (Blanco et al., 2022; Vandersluis et al., 2020). According to Hajizadeh et al., Al alloy hardness is between 32–52 HV (Hajizadeh et al., 2017). Therefore, all specimens have hardness still higher than Al alloy.

#### 4.3 OCP

Figure 3 shows the OCP measurement result of various casting samples in 0.9 % NaCl at room temperature. Generally, increased Zn content in the alloy promoted more negative potential,

which perfectly agrees with the Cocco et al. study (Cocco et al., 2016). Dridi et al. have found that  $E_{OCP}$  CuZn30 and CuZn39 are -0.578 and -0.604 V/MSE at 3 % NaCl, which means an increase in the Zn promoted to more negative potential (Dridi et al., 2020). Cu, Cu6Zn, Cu9Zn, and Cu12Zn samples have  $E_{OCP}$  potential at 1200 s measurement -0.014, -0.023, -0.027, and -0.032 V vs Ag/AgCl, respectively.

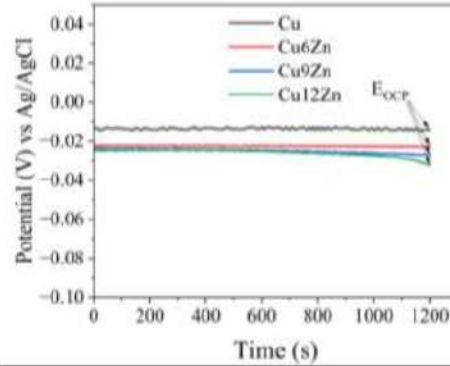


Fig. 3. OCP measurement of various casting samples.

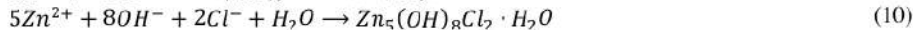
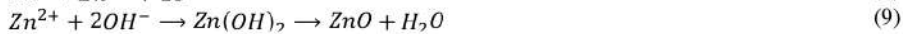
According to Figure 3, Cu, Cu6Zn, and Cu9Zn samples are steady at initial measurements until 1200 s, indicating that the protective layer formed has good protection. In contrast, the Cu12Zn sample is steady at initial measurements until 600 s, then moves in a more negative direction. These phenomena indicated that the formed protective layer had initially dissolved at 600 s; therefore, the measurement continuously moved forward in a negative direction until the measurement reached 1200 s.

#### 4.4 LSV

Eccrine sweat and saline-infused for humans are nearly 0.9 % of NaCl (Bond & Lieu, 2014; Tayyab et al., 2021). Therefore, LSV measurement was conducted in 0.9 % NaCl at room temperature. Luo et al. found Cu<sub>2</sub>O crystalline growth on the Cu surface when exposed to 0.9 % NaCl, while when exposed to pure water, Cu<sub>2</sub>O crystalline was not seen (Luo et al., 2020). Commonly, Cu<sub>2</sub>O crystallines are formed, which is preceded by the formation of CuCl when the specimen is tested in a chloride solution. Moreover, Zhang et al., in their study, found ZnO and Zn<sub>5</sub>Cl<sub>2</sub>(OH)<sub>8</sub>·H<sub>2</sub>O as corrosion products on top of Cu40Zn surfaces in a chloride environment (Zhang et al., 2016). The reaction of Cu in chloride solution is as follows (Milošev et al., 2024).



The reaction of Zn in chloride solution is as follows (Milošev et al., 2024).



LSV measurement results in 0.9 % NaCl can be seen in Figure 4.

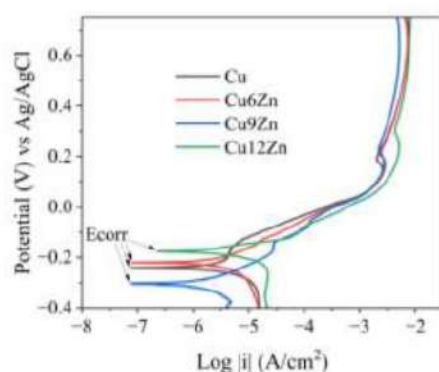


Fig. 4. LSV scans result of various casting samples.

According to Figure 4, corrosion  $E_{corr}$  and  $i_{corr}$  can be found using the Tafel extrapolation method. Moreover, the corrosion rate could be calculated by inserting  $i_{corr}$  into expression (1). Table 3 presented  $E_{corr}$ ,  $i_{corr}$ , and the corrosion rate of various casting samples. It appears  $E_{corr}$  is independent of Zn addition; however, Zn is dependent on  $i_{corr}$  and corrosion rate (except for the Cu12Zn sample). This behavior is probably due to a protective layer that was formed. Compared to the OCP result, it can be seen that the Cu12Zn sample continuously moves forward in a negative direction from 600 until 1200 s of measurement. Therefore, that sample has a higher  $i_{corr}$  and corrosion rate.

Table 3 - Corrosion parameters of various casting samples.

Sample name	$E_{corr}$ (V) vs Ag/AgCl	$i_{corr}$ (A/cm <sup>2</sup> )	Corrosion rate (mmpy)
Cu	-0.241	$4.42 \times 10^{-6}$	$5.13 \times 10^{-2}$
Cu6Zn	-0.220	$3.33 \times 10^{-6}$	$3.86 \times 10^{-2}$
Cu9Zn	-0.304	$2.15 \times 10^{-6}$	$2.49 \times 10^{-2}$
Cu12Zn	-0.175	$6.19 \times 10^{-6}$	$7.18 \times 10^{-2}$

Qu et al. have found that an increase in Zn content led to an increase in corrosion resistance, which perfectly agrees with the present study (except for Cu12Zn) (Qu et al., 2020). Milošev et al. investigated Cu, Cu10Zn, Cu40Zn, and Zn in 3 % NaCl and found  $i_{corr}$  after stabilized at 1 hour around 1.573, 1.456, and 2.114, and 5.21  $\mu\text{A}/\text{cm}^2$  respectively (Milošev et al., 2024). According to equation (1),  $i_{corr}$  strongly influences the corrosion rate. The more  $i_{corr}$ , the higher the corrosion rate. Moreover, a limitation in Zn content in the Cu alloy could influence the corrosion resistance. Presenting the Zn content  $\leq 11$  wt.% in the alloy could enhance the corrosion resistance; however, Zn of more than 10 wt.% could decrease corrosion resistance (Milošev et al., 2024).

According to Table 2, the Cu9Zn sample has the lowest microstrain than others. The measured microstrain could be associated with the sample's crystal defect (Soegijono et al., 2020). Based on Table 2, the Cu9Zn sample has the lowest microstrain, which confirms that the sample has the lowest corrosion rate. Moreover, the FCC sample with the preferred orientation of the (111) plane could offer a lower corrosion rate due to the highest surface atomic density (Jinlong et al., 2016; Soegijono et al., 2020). Compared to other samples, the Cu9Zn sample has the higher preferred orientation of the (111) plane. Even though the (111) plane of the Cu sample is the highest. Unfortunately, the (220) and (200) planes are still present and relatively high.

#### 4.5 Antibacterial Activity

Figure 5 shows the direct contact kill of *Staphylococcus aureus* and *Escherichia coli* after 24 hours of incubation. The present study focused on *Staphylococcus aureus*, but *Escherichia coli* was also used for comparison. There is no diffusion in the sample; therefore, the inhibition zone could not be seen.



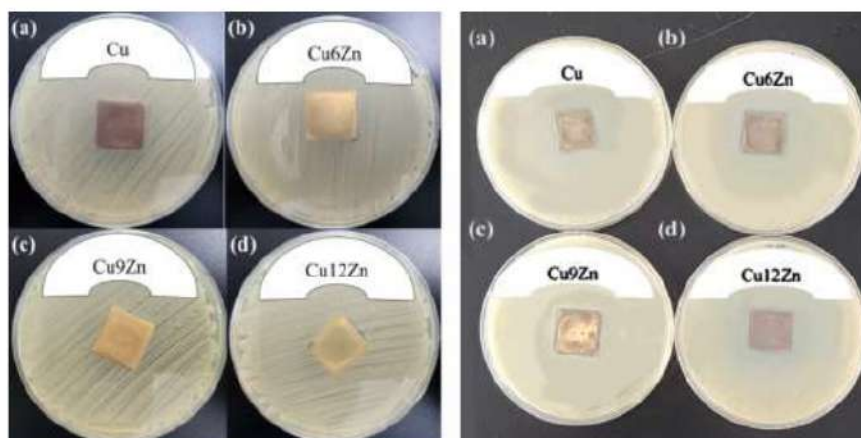


Fig. 5. Antibacterial activity test using *Staphylococcus aureus* (left) and *Escherichia coli* (right) (a) Cu, (b) Cu6Zn, (c) Cu9Zn, and (d) Cu12Zn.

Antibacterial activity after 24 hours of post-contact with various casting samples using *Staphylococcus aureus* and *Escherichia coli* can be seen in Figure 6. The removed sample places remain clear (with no regrowth) from bacterial activity. The antibacterial behavior was significantly influenced by Cu or Zn ions (Qu et al., 2020). Villapún et al. found that releasing Cu ions leads to the highest killing activity of *Staphylococcus aureus* (Villapún et al., 2016). Excess in the Cu ion could be bacteriostatic (Sabbouh et al., 2023). Moreover, Cu ions could be adsorbed on the cytoplasmic membrane surfaces, then penetrate the bacteria, react with sulfhydryl groups and cause the cell to die (Zeng et al., 2022). Furthermore, Cu ions could form hydroxyl groups in the presence of oxygen in nature, which could destroy cell membranes (Dou et al., 2022). Hutchings et al. stated that  $Zn^{2+}$  successfully inhibits the growth of *S. epidermidis* (Hutchings et al., 2021). This behavior is associated with the generation of reactive oxygen or the formation of (Zhang et al., 2021).

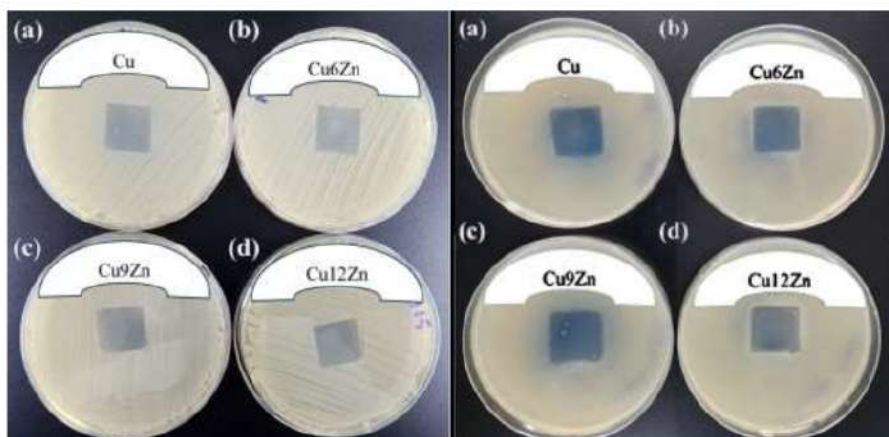


Fig. 6. Antibacterial activity after 24 hours of post-contact (regrowth assessment) towards *Staphylococcus aureus* (left) and *Escherichia coli* (right) (a) Cu, (b) Cu6Zn, (c) Cu9Zn, and (d) Cu12Zn

Figure 7 shows the fluid contact test of *Staphylococcus aureus* and *Escherichia coli*. The orientation of the test materials is mapped within the yellow box. For the Cu6Zn sample, *Escherichia coli* was killed on the 3<sup>rd</sup> hour. However, there is no significant reduction within the

fluid because there are no diffusible materials. Also, there is no visible growth after 3<sup>rd</sup> hour for the fluid in contact with the metal.

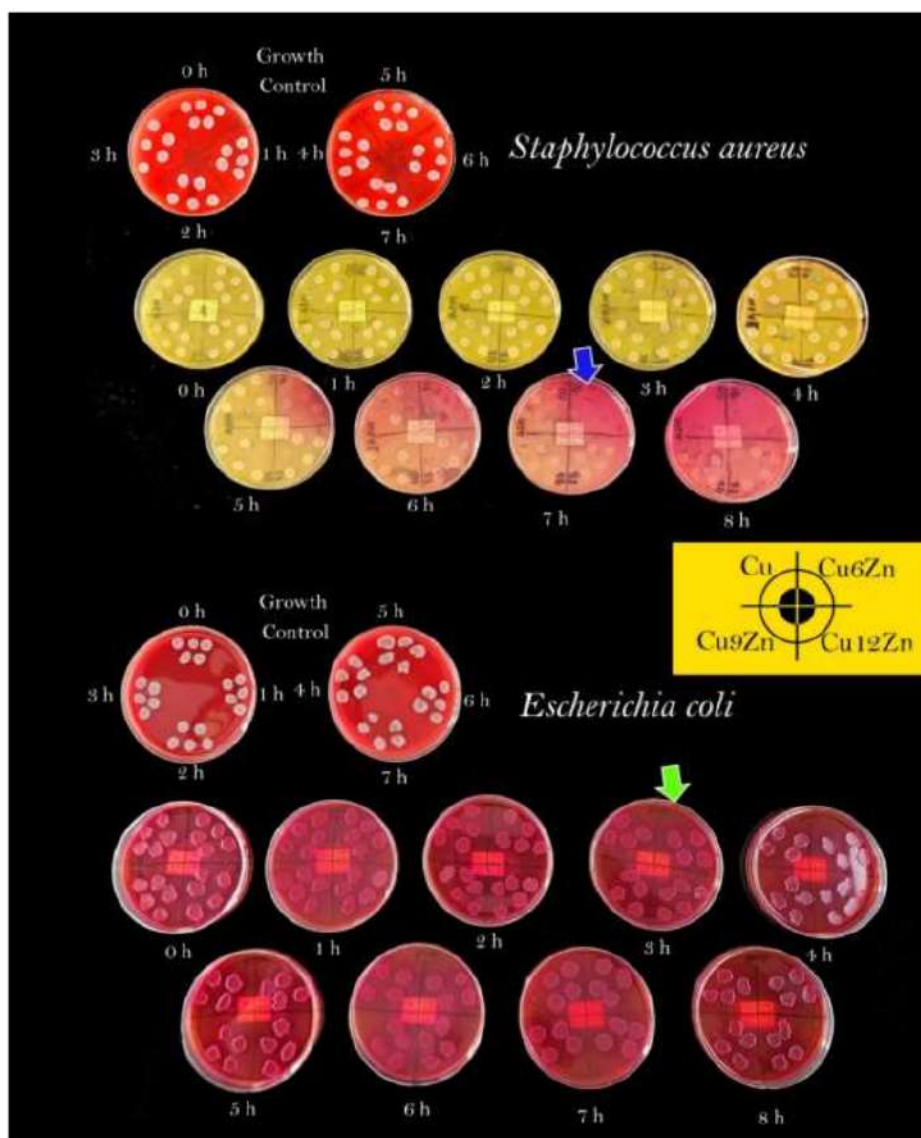


Fig. 7. Fluid contact test of *Staphylococcus aureus* and *Escherichia coli*

Moreover, it should be noted that the reduction of the colony is significant in the 7<sup>th</sup> hour for *Staphylococcus aureus* (blue arrow), but for *Escherichia coli*, the inhibition of *Escherichia coli* growth is shown within the 3<sup>rd</sup> hour of contact (green arrow), for Cu6Zn sample. The reduction of colonies is significant on the surface of the metal. While on the remaining fluid, the reduction is insignificant until 8 hours. This behavior is because *Staphylococcus aureus* and *Escherichia coli* have different membrane structures and thick cell walls, therefore could inhibit ion exchange and restrain the antibacterial effect of Cu and or Zn ions (Di et al., 2022). Cu killing is more effective in Gram-negative bacteria (e.g., *Escherichia coli*) because peptidoglycan affects the cell's susceptibility. The thicker the peptidoglycan layer, the harder it became for the Cu ions

to reach the membrane (Soltani et al., 2020; Khafa et al., 2023). Therefore, *Escherichia coli* was killed in the 3<sup>rd</sup> hour. Another reason Cu6Zn has better antibacterial performance than others is probably due to its smaller crystallite size. Researchers found that smaller crystallite sizes promote the enhancement of antibacterial effects (Syamsuir et al., 2023). This behavior is attributed to an increase in surface area due to the crystallite size (Sangeetha et al., 2015). The Cu6Zn sample could be used as an alternative material for medical equipment in ambulances.

## 5. Conclusion

CuZn has been successfully fabricated. XRD confirmed that CuZn alloy has a single alpha phase with an FCC crystal structure. The rise of the Zn content in the alloy led to a decrease in the hardness due to an increase in crystallite size and led to a shift to more negative OCP potential at 1200 s measurement. Moreover, the rise of the Zn content to 9 wt.% decreased the corrosion rate. It appears there is a limitation in Zn content in the copper alloy that influences the corrosion rate, as shown when Zn content around 12 wt. % is promoted to increase the corrosion rate. Antibacterial activity observation found that all samples had no diffusion. Moreover, 24-hour post-contact observation found that sample places removed from the sample remained clear of bacteria. The Cu6Zn has better antibacterial performance than others due to the smallest crystallite size. According to the fluid contact test, the reduction of the colony of *Staphylococcus aureus* is significant in the 7<sup>th</sup> hour. The inhibition of *Escherichia coli* growth is also shown within the 3<sup>rd</sup> hour of contact. This behavior is because *Staphylococcus aureus* and *Escherichia coli* have different membrane structures and thick cell walls, therefore, could inhibit ion exchange and restrain the antibacterial effect of Cu and or Zn ions.

## Acknowledgement

This research is under financial support from the Ministry of Education, Culture, Research and Technology Indonesia with contract number 832/LL3/AL.04/2024 and 171/A/LPPM-P/USAKTI/VI/2024.

## References

- Abed, K. M., & Dawood, N. M. (2022). Impacts of Tin and Germanium on Corrosion and Erosion-Corrosion Behavior of 60Cu-40Zn alloys. *AIP Conference Proceedings*, 2660, 020131. <https://doi.org/10.1063/5.0108474>
- Akhyar, Iqbal, Ali, N., & Husin, H. (2023). Effect of variations in pouring temperature on tensile strength of CuZn cast alloys. *Materials Letters: X*, 17, 100182. <https://doi.org/10.1016/j.mlbox.2023.100182>
- Augustin, A., Huilgol, P., Udupa, K. R., & Bhat K, U. (2016). Effect of current density during electrodeposition on microstructure and hardness of textured Cu coating in the application of antimicrobial Al touch surface. *Journal of the Mechanical Behavior of Biomedical Materials*, 63, 352–360. <https://doi.org/10.1016/j.jmbbm.2016.07.013>
- Azizian, F., Naffakh-Moosavy, H., & Bagheri, F. (2024). The role of Cu addition in the metallurgical features, mechanical properties, and cytocompatibility of cardiovascular stents biodegradable Zn-based alloy. *Intermetallics*, 164, 108106. <https://doi.org/10.1016/j.intermet.2023.108106>
- Baker, L. B., & Wolfe, A. S. (2020). Physiological mechanisms determining eccrine sweat composition. *European Journal of Applied Physiology*, 120(4), 719–752. <https://doi.org/10.1007/s00421-020-04323-7>
- Bhavsar, V., & Bali, S. C. (2023). Effect of Compressed Natural Gas (CNG) on corrosion behaviour of brass valve of CNG cylinder. *Engineering Failure Analysis*, 149, 107268. <https://doi.org/10.1016/j.engfailanal.2023.107268>
- Blanco, D., Mar, E., & Mar, R. (2022). Titanium Alloys Applied to the Transport Sector : A Review. *Metals*, 12(9), 1–21. <https://doi.org/10.3390/met12010009>
- Bond, J. W., & Lieu, E. (2014). Electrochemical behaviour of brass in chloride solution concentrations found in eccrine fingerprint sweat. *Applied Surface Science*, 313, 455–461. <https://doi.org/10.1016/j.apsusc.2014.06.005>
- Chen, L., Ma, R., Dong, J., Chen, S., Li, C., Ma, C., Bian, G., & Wang, C. (2024). A multi-ion



- transport model of Cu-Zn-Fe trimetallic couple in near-neutral NaCl solution. *Corrosion Science*, 239, 112414. <https://doi.org/10.1016/j.corsci.2024.112414>
- Clement, A., & Auger, T. (2023). An EAM potential for  $\alpha$ -brass copper-zinc alloys: application to plasticity and fracture. *Modelling and Simulation in Materials Science and Engineering*, 31(1), 015004. <https://doi.org/10.1088/1361-651X/aca4ec>
- Cocco, F., Fantauzzi, M., Elsener, B., & Rossi, A. (2016). Dissolution of brass alloys naturally aged in neutral solutions-an electrochemical and surface analytical study. *RSC Advances*, 6(93), 90654–90665. <https://doi.org/10.1039/c6ra18200c>
- Di, T., Xu, Y., Liu, D., & Sun, X. (2022). Microstructure, Mechanical Performance and Anti-Bacterial Activity of Degradable Zn-Cu-Ag Alloy. *Metals*, 12(9), 1–13. <https://doi.org/10.3390/met12091444>
- Dou, X., Chen, Y., & Shi, H. (2022). CuBi2O4/BiOBr composites promoted PMS activation for the degradation of tetracycline: S-scheme mechanism boosted Cu<sup>2+</sup>/Cu<sup>+</sup> cycle. *Chemical Engineering Journal*, 431(P2), 134054. <https://doi.org/10.1016/j.cej.2021.134054>
- Dridi, A., Dhoubi, L., Hihn, J. Y., Berçot, P., Rezrazi, E. M., Sassi, W., & Rouge, N. (2020). Analytical Study of CuZn 30 and CuZn 39 Brass Surfaces in 3% NaCl Solution Under Polarization. *Chemistry Africa*, 3(3), 735–747. <https://doi.org/10.1007/s42250-020-00182-z>
- Du, M., Zhao, W., Ma, R., Xu, H., Zhu, Y., Shan, C., Liu, K., Zhuang, J., & Jiao, Z. (2021). Visible-light-driven photocatalytic inactivation of *S. aureus* in aqueous environment by hydrophilic zinc oxide (ZnO) nanoparticles based on the interfacial electron transfer in *S. aureus*/ZnO composites. *Journal of Hazardous Materials*, 418, 126013 Contents. <https://doi.org/10.1016/j.jhazmat.2021.126013>
- Ezequiel, M., Proriot Serre, I., Auger, T., Héripé, E., Hadjem-Hamouche, Z., & Perriere, L. (2024). The liquid metal embrittlement of a reactive system at room temperature:  $\alpha$ -brasses in contact with the liquid eutectic Ga-In. *Engineering Failure Analysis*, 164, 108694. <https://doi.org/10.1016/j.engfailanal.2024.108694>
- Gao, P., Ren, Y., Qian, S., He, Y., & Shen, D. (2021). Evolution of microstructure and electrochemical corrosion behavior of CuZn-based alloys induced by cold rolling. *Journal of Materials Research and Technology*, 15, 360–368. <https://doi.org/10.1016/j.jmrt.2021.08.035>
- García-Mintegui, C., Córdoba, L. C., Buxadera-Palomero, J., Marquina, A., Jiménez-Piqué, E., Ginebra, M. P., Cortina, J. L., & Pegueroles, M. (2021). Zn-Mg and Zn-Cu alloys for stenting applications: From nanoscale mechanical characterization to in vitro degradation and biocompatibility. *Bioactive Materials*, 6(12), 4430–4446. <https://doi.org/10.1016/j.bioactmat.2021.04.015>
- Hajizadeh, K., Ejtemaei, S., & Eghbali, B. (2017). Microstructure, hardness homogeneity, and tensile properties of 1050 aluminum processed by constrained groove pressing. *Applied Physics A: Materials Science and Processing*, 123(8), 1–9. <https://doi.org/10.1007/s00339-017-1123-y>
- Heidarzadeh, A., Javidani, M., & St-Georges, L. (2022). Crystallographic Orientation Relationship between  $\alpha$  and  $\beta$  Phases during Non-Equilibrium Heat Treatment of Cu-37 wt. % Zn Alloy. *Crystals*, 12(1), 97. <https://doi.org/10.3390/cryst12010097>
- Hendrawan, C. N., Setyani, A., Pertiwi, D. R. K., & Sofyan, B. T. (2021). Effect of 9wt% Mn addition on cold rolling and annealing behaviour of Cu-31Zn alloy. *Materials Today: Proceedings*, 46, 3346–3351. <https://doi.org/10.1016/j.matpr.2020.11.476>
- Huang, S. J., Li, C., Feng, J. H., Selvaraju, S., & Subramani, M. (2024). Mechanical and Corrosion Tests for Magnesium–Zinc/Ti-6Al-4V Composites by Gravity Casting. *Materials*, 17(8), 1836. <https://doi.org/10.3390/ma17081836>
- Hutchings, C., Yair, Z. P., Reifen, R., & Shemesh, M. (2021). Antimicrobial effect of zn<sup>2+</sup> ions governs the microbial quality of donor human milk. *Foods*, 10(3), 1–12. <https://doi.org/10.3390/foods10030637>
- Iqbal, Ali, N., Husin, H., Akhyar, Khairil, & Farhan, A. (2021). Differences in Pour Temperature Affect Hardness Properties of CuZn Brass Alloy through Metal Casting. *IOP Conference Series: Materials Science and Engineering*, 1082(1), 012001.

- <https://doi.org/10.1088/1757-899x/1082/1/012001>
- Jinlong, L., Tongxiang, L., & Chen, W. (2016). Effect of electrodeposition temperature on grain orientation and corrosion resistance of nanocrystalline pure nickel. *Journal of Solid State Chemistry*, 240, 109–114. <https://doi.org/10.1016/j.jssc.2016.05.025>
- Karahan, I. H., & Özdemir, R. (2014). Effect of Cu concentration on the formation of Cu 1-x Zn x shape memory alloy thin films. *Applied Surface Science*, 318, 100–104. <https://doi.org/10.1016/j.apsusc.2014.01.119>
- Liu, P., Hu, J. ying, Li, H. xue, Sun, S. yu, & Zhang, Y. bin. (2020). Effect of heat treatment on microstructure, hardness and corrosion resistance of 7075 Al alloys fabricated by SLM. *Journal of Manufacturing Processes*, 60, 578–585. <https://doi.org/10.1016/j.jmapro.2020.10.071>
- Luo, J., Hein, C., Pierson, J. F., & Mücklich, F. (2020). Sodium chloride assists copper release, enhances antibacterial efficiency, and introduces atmospheric corrosion on copper surface. *Surfaces and Interfaces*, 20, 100630. <https://doi.org/10.1016/j.surfin.2020.100630>
- Milošev, I., Taheri, P., Kapun, B., Kozlica, D. K., Mol, A., & Kokalj, A. (2024). The effect of molecular structure of imidazole-based compounds on corrosion inhibition of Cu, Zn, and Cu-Zn alloys. *Corrosion Science*, 127870. <https://doi.org/10.1016/j.corsci.2024.112328>
- Morath, L., Rahim, S. A., Baker, C., Anderson, D., Hinds, M., Sikora-Jasinska, M., Oujiri, L., Leyssens, L., Kerckhofs, G., Pyka, G., Oliver, A. A., Drelich, J. W., & Goldman, J. (2024). The biological effects of copper alloying in Zn-based biodegradable arterial implants. *Biomaterials Advances*, November, 124658. <https://doi.org/10.1016/j.bioadv.2024.214112>
- Mousavi, S. E., Sonboli, A., Naghshehkesh, N., Meratian, M., Salehi, A., & Sanayei, M. (2020). Different behavior of alpha and beta phases in a Low Stacking Fault Energy copper alloy under severe plastic deformation. *Materials Science and Engineering: A*, 788, 139550. <https://doi.org/10.1016/j.msea.2020.139550>
- Nikhil, Singh, M. K., Ji, G., & Prakash, R. (2021). Investigation on the effects of cooling rate on surface Texture, corrosion behaviour and hardness of pure copper. *Materials Today: Proceedings*, 47(19), 6693–6695. <https://doi.org/10.1016/j.matpr.2021.05.115>
- Nnakwo, K. C., Osakwe, F. O., Ugwuanyi, B. C., Oghenekowho, P. A., Okeke, I. U., & Maduka, E. A. (2021). Grain characteristics, electrical conductivity, and hardness of Zn-doped Cu–3Si alloys system. *SN Applied Sciences*, 3(11), 829. <https://doi.org/10.1007/s42452-021-04784-1>
- Nuryadi, N., Sudarsono, B., & Asistiyasari, A. (2020). Effect of Moisture Content of Green Sand on The Casting Defects. *Journal of Applied Engineering and Technological Science*, 4(1), 586–598.
- Özdemir, R., & Karahan, I. H. (2014). Electrodeposition and properties of Zn, Cu, and Cu 1-x Zn x thin films. *Applied Surface Science*, 318, 314–318. <https://doi.org/10.1016/j.apsusc.2014.06.188>
- Pietrocola, G., Campoccia, D., Motta, C., Montanaro, L., Arciola, C. R., & Speziale, P. (2022). Colonization and Infection of Indwelling Medical Devices by Staphylococcus aureus with an Emphasis on Orthopedic Implants. *International Journal of Molecular Sciences*, 23(11), 5958. <https://doi.org/10.3390/ijms23115958>
- Qu, X., Yang, H., Jia, B., Yu, Z., Zheng, Y., & Dai, K. (2020). Biodegradable Zn–Cu alloys show antibacterial activity against MRSA bone infection by inhibiting pathogen adhesion and biofilm formation. *Acta Biomaterialia*, 117, 400–417. <https://doi.org/10.1016/j.actbio.2020.09.041>
- Riaz, M., Najam, M., Imtiaz, H., Bashir, F., & Hussain, T. (2024). Structural and biological analysis of Zn–Cu based biodegradable alloys for orthopedic application. *Materials Chemistry and Physics*, 312, 128618. <https://doi.org/10.1016/j.matchemphys.2023.128618>
- Sabbouh, M., Nikitina, A., Rogacheva, E., Nebalueva, A., Shilovskikh, V., Sadovnichii, R., Koroleva, A., Nikolaev, K., Kraeva, L., Ulasevich, S., & Skorb, E. (2023). Sonochemical fabrication of gradient antibacterial materials based on Cu-Zn alloy. *Ultrasonics Sonochemistry*, 92, 106247. <https://doi.org/10.1016/j.ultsonch.2022.106247>
- Sangeetha, R., Muthukumar, S., & Ashokkumar, M. (2015). Structural, optical, dielectric and antibacterial studies of Mn doped Zn<sub>0.96</sub>Cu<sub>0.04</sub>O nanoparticles. *Spectrochimica Acta -*

- Part A: *Molecular and Biomolecular Spectroscopy*, 144, 1–7. <https://doi.org/10.1016/j.saa.2015.02.056>
- Shahriyari, F., Shaeri, M. H., Dashti, A., Zarei, Z., Noghani, M. T., Cho, J. H., & Djavanroodi, F. (2022). Evolution of mechanical properties, microstructure and texture and of various brass alloys processed by multi-directional forging. *Materials Science and Engineering: A*, 831, 142149. <https://doi.org/10.1016/j.msea.2021.142149>
- Situmorang, E. M. H., Henniuriyama, V., & Soegijono, B. (2019). Oligodynamic Cu-Zn composite fabricated by powder metallurgy method. *Journal of Physics: Conference Series*, 1191(1). <https://doi.org/10.1088/1742-6596/1191/1/012044>
- Soegijono, B., Susetyo, F. B., Yusmaniar, & Fajrah, M. C. (2020). Electrodeposition of paramagnetic copper film under magnetic field on paramagnetic aluminum alloy substrates. *E-Journal of Surface Science and Nanotechnology*, 18, 281–288. <https://doi.org/10.1380/EJSSNT.2020.281>
- Soltani, S., Akhbari, K., & White, J. (2020). Synthesis, crystal structure, magnetic, photoluminescence and antibacterial properties of dinuclear Copper(II) complex. *Journal of Molecular Structure*, 1214, 128233. <https://doi.org/10.1016/j.molstruc.2020.128233>
- Strzpek, P., Marnala, A., Zasadzińska, M., Franczak, K., & Jurkiewicz, B. (2019). Research on the drawing process of Cu and CuZn wires obtained in the cryogenic conditions. *Cryogenics*, 100, 11–17. <https://doi.org/10.1016/j.cryogenics.2019.03.007>
- Syamsuir, Susetyo, F. B., Soegijono, B., Yudianto, S. D., Basori, Ajiriyanto, M. K., Edbert, D., Situmorang, E. U. M., Nanto, D., & Rosyidan, C. (2023). Rotating-Magnetic-Field-Assisted Electrodeposition of Copper for Ambulance Medical Equipment. *Automotive Experiences*, 6(2), 290–302. <https://doi.org/10.31603/ae.9067>
- Tajik, S., Najar-Peerayeh, S., & Bakhshi, B. (2020). Hospital clones of Pantone-Valentine leukocidin-positive and methicillin-resistant *Staphylococcus aureus* circulating in the Tehran community. *Journal of Global Antimicrobial Resistance*, 22, 177–181. <https://doi.org/10.1016/j.jgar.2019.12.010>
- Tayyab, K. Bin, Farooq, A., Alvi, A. A., Nadeem, A. B., & Deen, K. M. (2021). Corrosion behavior of cold-rolled and post heat-treated 316L stainless steel in 0.9wt% NaCl solution. *International Journal of Minerals, Metallurgy and Materials*, 28(3), 440–449. <https://doi.org/10.1007/s12613-020-2054-8>
- Vandersluis, E., Machin, A., Perovic, D., & Ravindran, C. (2020). Failure Analysis of an Ambulance Cathode Ray Tube Monitor Bracket. *Journal of Failure Analysis and Prevention*, 20(1), 23–33. <https://doi.org/10.1007/s11668-020-00804-1>
- Viegas, C., Sousa, P., Dias, M., Caetano, L. A., Ribeiro, E., Carolino, E., Twańżek, M., Kosicki, R., & Viegas, S. (2021). Bioburden contamination and *Staphylococcus aureus* colonization associated with firefighter's ambulances. *Environmental Research*, 197, 111125. <https://doi.org/10.1016/j.envres.2021.111125>
- Villapún, V. M., Dover, L. G., Cross, A., & González, S. (2016). Antibacterial metallic touch surfaces. *Materials*, 9(9), 1–23. <https://doi.org/10.3390/ma9090736>
- Wang, X., Su, H., Xie, Y., Wang, J., Feng, C., Li, D., & Wu, T. (2023). Atmospheric corrosion of T2 copper and H62 brass exposed in an urban environment. *Materials Chemistry and Physics*, 299, 127487. <https://doi.org/10.1016/j.matchemphys.2023.127487>
- Widyastuti, Rochiem, R., Fellicia, D. M., Adrinanda, C. F. N., & Wibowo, A. P. (2023). Mechanical Properties, Microstructural, and Deep Drawing Formability Analysis on the Annealed CuZn35 Brass Alloy for Cartridge Application. *Key Engineering Materials*, 939, 31–37. <https://doi.org/10.4028/p-21x8y5>
- Khafa, S., Olivieri, L., Di Nicola, C., Pettinari, R., Pettinari, C., Tombesi, A., & Marchetti, F. (2023). Copper and Zinc Metal–Organic Frameworks with Bipyrazole Linkers Display Strong Antibacterial Activity against Both Gram+ and Gram– Bacterial Strains. *Molecules*, 28(16), 6160. <https://doi.org/10.3390/molecules28166160>
- Yin, M. yang, Li, Z., Xiao, Z., Pang, Y., Li, Y. ping, & Shen, Z. yan. (2021). Corrosion behavior of Cu–Al–Mn–Zn–Zr shape memory alloy in NaCl solution. *Transactions of Nonferrous Metals Society of China (English Edition)*, 31(4), 1012–1022. [https://doi.org/10.1016/S1003-6326\(21\)65557-7](https://doi.org/10.1016/S1003-6326(21)65557-7)

- 
- Zeng, J., Geng, X., Tang, Y., Xiong, Z. C., Zhu, Y. J., & Chen, X. (2022). Flexible photothermal biopaper comprising Cu<sup>2+</sup>-doped ultralong hydroxyapatite nanowires and black phosphorus nanosheets for accelerated healing of infected wound. *Chemical Engineering Journal*, 437, 135347. <https://doi.org/10.1016/j.cej.2022.135347>
- Zhang, E., Zhao, X., Hu, J., Wang, R., Fu, S., & Qin, G. (2021). Antibacterial metals and alloys for potential biomedical implants. *Bioactive Materials*, 6(8), 2569–2612. <https://doi.org/10.1016/j.bioactmat.2021.01.030>
- Zhang, X., Liu, X., Odnevall Wallinder, I., & Leygraf, C. (2016). The protective role of hydrozincite during initial corrosion of a Cu<sub>40</sub>Zn alloy in chloride-containing laboratory atmosphere. *Corrosion Science*, 103, 20–29. <https://doi.org/10.1016/j.corsci.2015.10.027>
- Ziat, Y., Hammi, M., Laghlimi, C., & Moutcine, A. (2020). Investment casting of leaded brass: Microstructure micro-hardness and corrosion protection by epoxy coating. *Materialia*, 12, 100794 Contents. <https://doi.org/10.1016/j.mtla.2020.100794>

# EFFECT OF ZINC ADDITION IN COPPER TO STRUCTURE, HARDNESS, CORROSION, AND ANTIBACTERIAL ACTIVITY

---

ORIGINALITY REPORT

---

20%  
SIMILARITY INDEX

12%  
INTERNET SOURCES

11%  
PUBLICATIONS

4%  
STUDENT PAPERS

---

MATCH ALL SOURCES (ONLY SELECTED SOURCE PRINTED)

---

1%  
★ m.riunet.upv.es  
Internet Source

---

Exclude quotes      Off  
Exclude bibliography      Off

Exclude matches      Off